AFCRL 68-0589

EVALUATION OF SEISMIC INSTRUMENTS

AND

BASIC RESEARCH ON SEISMIC WAVE PROPAGATION

John G. Hogan, John F. Devane, S.J.,
Thomas P. Foley, Joseph J. Blaney,
William E. Haynes, Robert E. Hansen

Trustees of Boston College
Chestnut Hill, Massachusetts 02167

Contract No. AF19(628)6067

Project No. 8652

Task No. 865207

Work Unit No. 86520701

FINAL REPORT

Period Covered: June 1, 1966 - August 31, 1968

October 1968

Prepared for

AIR FORCE CAMBRIDGE RESEARCH LABORATORIES
OFFICE OF AEROSPACE RESEARCH
UNITED STATES AIR FORCE
BEDFORD, MASSACHUSETTS 01730

WORK SPONSORED BY ADVANCED RESEARCH PROJECTS AGENCY

PROJECT VELA-UNIFORM

ARPA Order No. 292

Project Code No. 8100 Task 2

AFCRL 68-0589

EVALUATION OF SEISMIC INSTRUMENTS

AND

BASIC RESEARCH ON SEISMIC WAVE PROPAGATION

John G. Hogan, John F. Devane, S.J.,
Thomas P. Foley, Joseph J. Blaney,
William E. Haynes, Robert E. Hansen

Trustees of Boston College
Chestnut Hill, Massachusetts 02167

Contract No. AF19(628)6067

Project No. 8652

Task No. 865207

Work Unit No. 86520701

FINAL REPORT

Period Covered: June 1, 1966 - August 31, 1968

October 1968

Prepared for

AIR FORCE CAMBRIDGE RESEARCH LABORATORIES
OFFICE OF AEROSPACE RESEARCH
UNITED STATES AIR FORCE
BEDFORD, MASSACHUSETTS 01730

WORK SPONSORED BY ADVANCED RESEARCH PROJECTS AGENCY

PROJECT VELA-UNIFORM

ARPA Order No. 292

Project Code No. 8100 Task 2

ABSTRACT

Seismometer test procedures are presented. Results of the tests performed on Electro-Tech's model EV17 seismometers used in the portable seismic detection system are detailed.

The results of frequency response tests performed on the portable seismic detection system are presented. Changes and modifications of the portable seismic detection system are described.

Equipment additions to the Data Analysis Laboratory are described. A brief discussion of a program used to process data taken with the portable seismic detection system is given.

A description of a quartz fiber tiltmeter and gravimeter developed during this contract is presented.

LIST OF CONTENTS

LIST OF FIGURES

LIST OF FIGURES (Cont.)

LIST OF TABLES

CHAPTER I

PORTABLE SEISMIC DETECTION SYSTEM

1. Calibration Circuit - Telemetry Packages

The calibrate circuit of the telemetry packages consists of a current source connected through a relay to an EV17 seismometer. The amplitude of the calibrate signal is controlled by a 6db per step 0-60db attenuator. The magnitude of the calibration current is related to milli-microns of earth motion through the motor constants of the EV17 seismometers.

The original design of the telemetry packages provided only for manual operation of the calibration circuit. Manual operation has two difficulties associated with it. First, pulse width in the manual mode cannot be accurately controlled. Second, calibration pulses cannot be applied to the telemetry system when the system is operating unattended. To solve these problems a calibration circuit which controls the pulse width and the pulse repetition rate was designed and installed.

The circuit uses a light activated monostable multivibrator to actuate a relay driver which closes the calibration relay. Once every fifteen minutes ($\pm$ 0.9 seconds) light is passed through a cutout in a motor driven wheel. The change in the transmitted

light level is sensed by a photocell and detected by a Schmitt trigger. The differentiated and clipped output pulse from the Schmitt trigger drives the monostable multivibrator. The duration of the multivibrator's unstable state determines the width of the calibration pulse.

A schematic of the calibration circuit is shown in Figure 1. The dc motor, blocking wheel, and light source are not shown.

2. DC - DC Converters for Transmitter and Receiver Packages

The initial design of the transmitter and receiver packages called for the use of six separate voltage levels. Elementary consideration of items such as discharge rate, cost of six separate types of batteries, and charging requirements indicated the inherent advantage of using a single supply voltage. Accordingly the transmitter and receiver packages were modified to incorporate regulators and dc to dc converters which would allow the use of a single supply voltage.

The regulators used belong to TECHNIPOWER'S CM line. The converters used belong to TECHNIPOWER'S CF line. The conversion efficiency of the units lies between 65% and 75%.

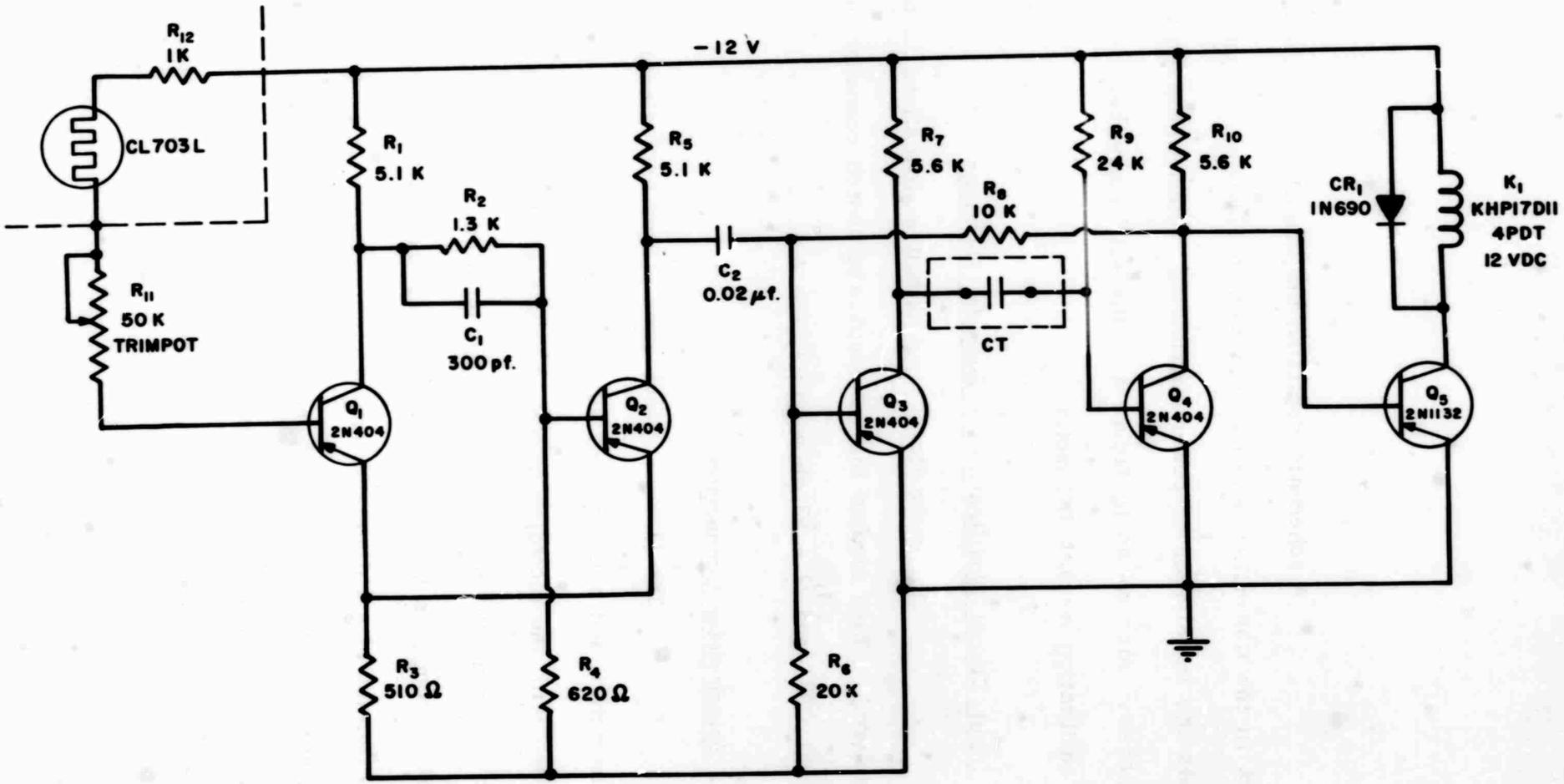

CALIBRATION CIRCUIT TRANSMITTER PACKAGE.

FIGURE 1

A schematic depicting the installation of these units in the transmitter package is shown in Figure 2. Figure 3 shows the installation of power distribution system in the receiver packages. Also shown in Figure 3 is the $+25^{V}$ connection for the calibration circuits DC motor.

3. Input Circuit Modifications - Recorder Packages

There are three input circuit modifications to be considered. They involve the connector and switch combinations J1 - S1, S2, and J2 - S3 shown in Figure 4.

3.A. Seismometer Connection

The J1 - S1 combination allows both single coil seismometers and seismometers with a separate calibration coil to be used with the recording packages. If a single coil seismometer is to be used, S1 must be in the down position. The input signal is taken from pins E - D of J1 and passes through the calibrator. Upon receipt of a calibrate command, the calibrator injects a calibrate current into the seismometer. At the expiration of the preselected calibration period, the current is removed. The motion of the seismometer mass under the action of the calibrate current

appears as a calibration pulse. If a dual coil seismometer is employed, S1 must be placed in the up position. The input signal then is taken from pins A - B of J1, and is sent directly to the parametric amplifiers. Pins E - D are again connected to the calibrate unit but the calibrate unit is disconnected from the parametric amplifiers. The calibrate procedure is the same as for single coil instruments except that the calibrate current is applied to the seismometer's calibrate coil and the calibration pulse is taken off the seismometer's sense coil.

3.3 Seismometer Response Modification

The switch S2 allows the seismometer to be shunted by one of four capacitors. The purpose of the capacitive shunting is to attenuate out of band high frequency noise. High frequency attenuation is required because the parametric amplifier has a larger bandpass than the rest of the system and can be saturated by high frequency cultural noise which will not be passed by the rest of the system and thus will not appear on playback. The effect of adding a capacitive shunt will be to increase the effective mass of the seismometer.

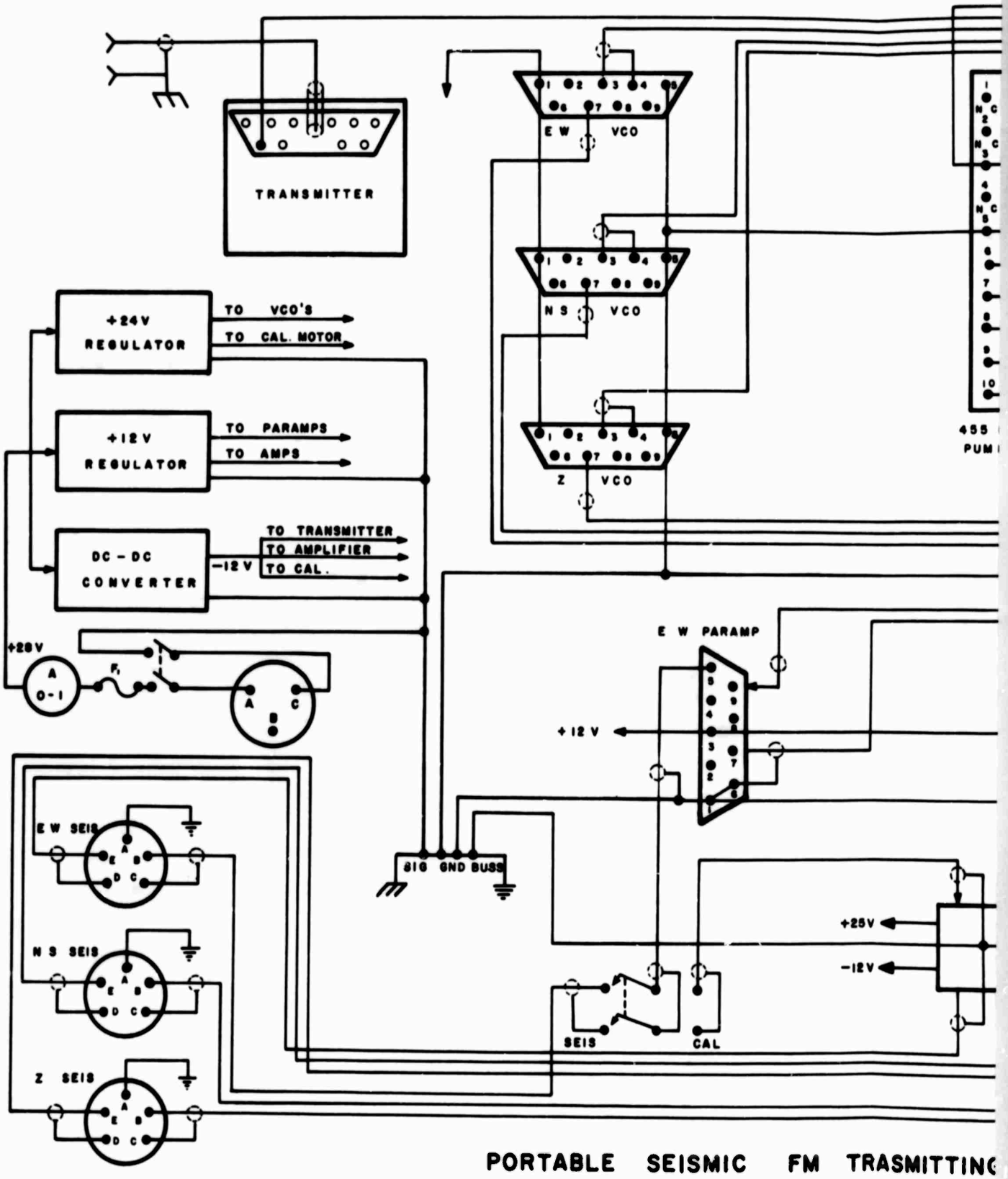

PORTABLE SEISMIC FM TRASMITTING

FIGURE 2

A

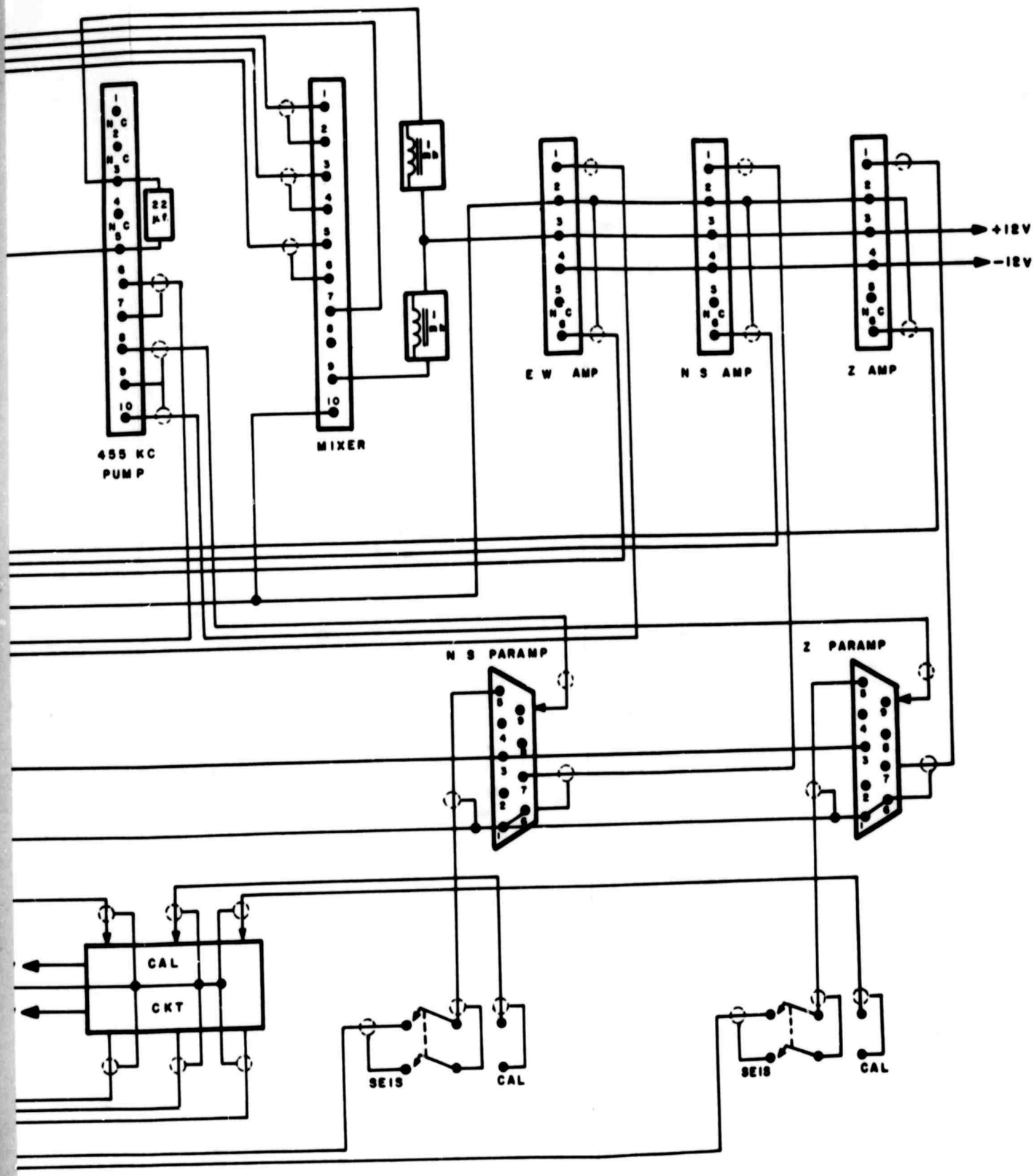

RASMITTING STATION (BOTTOM VIEW)

GURE 2

B

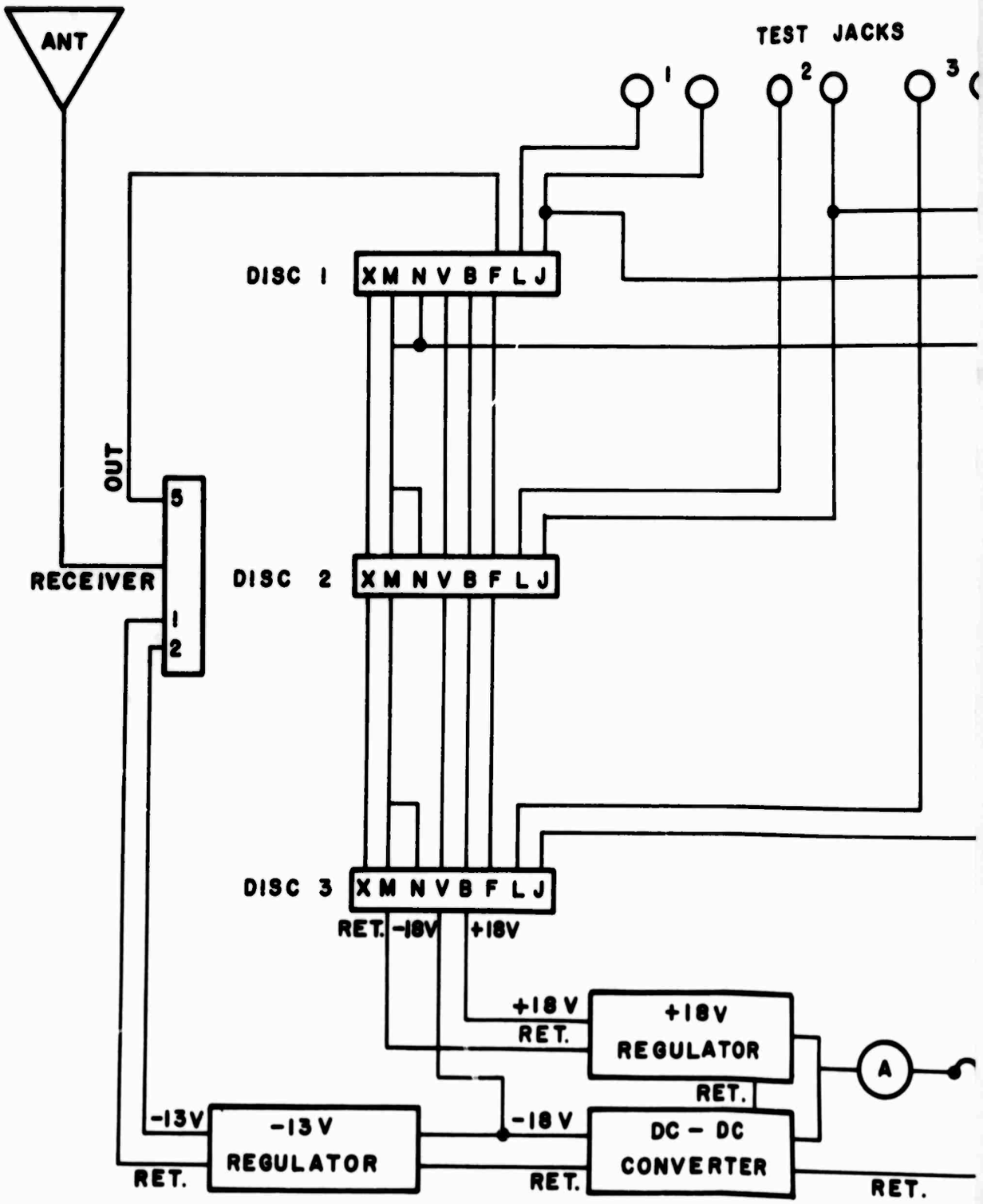

PORTABLE SEISMIC RECEIVING

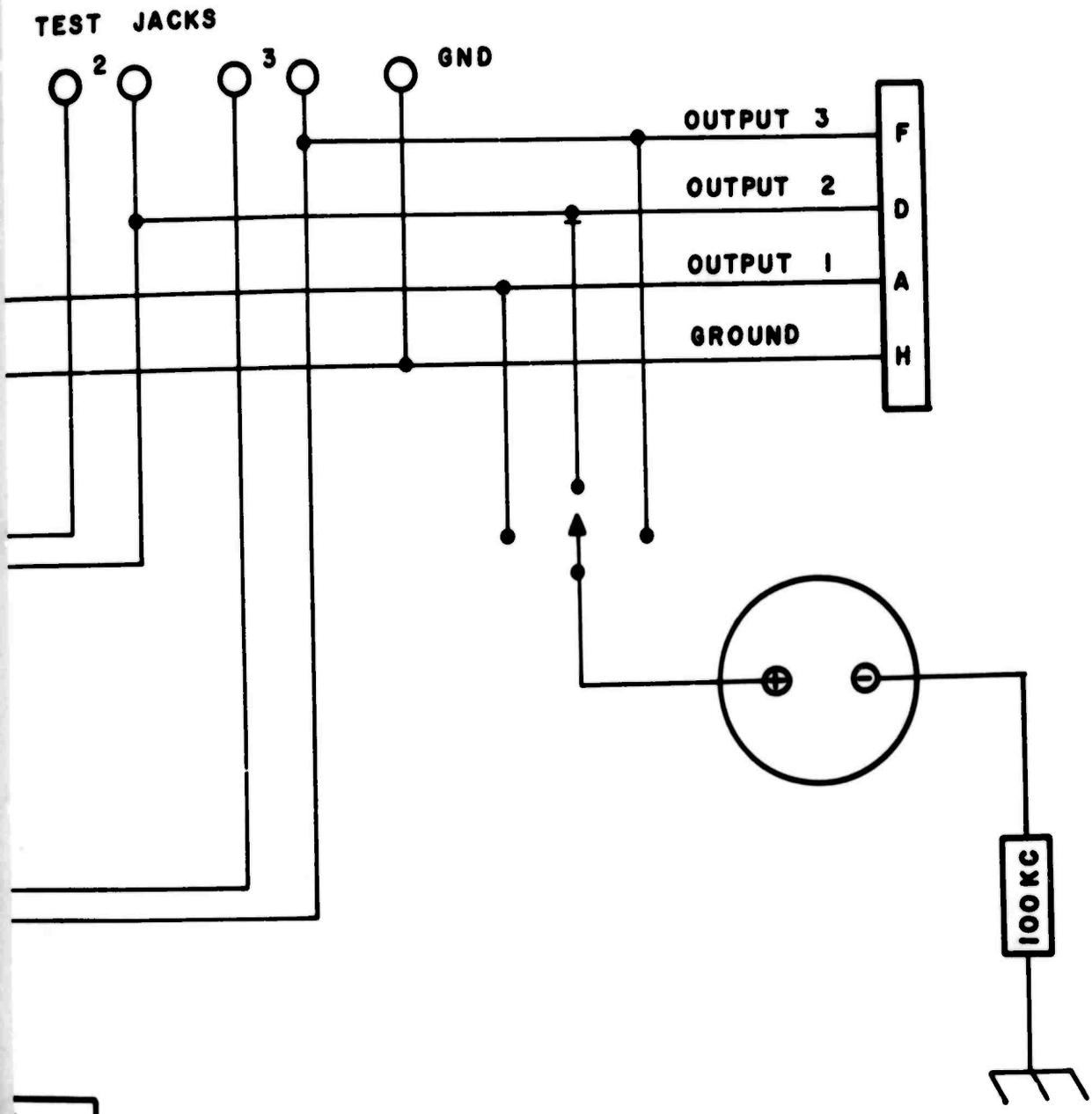

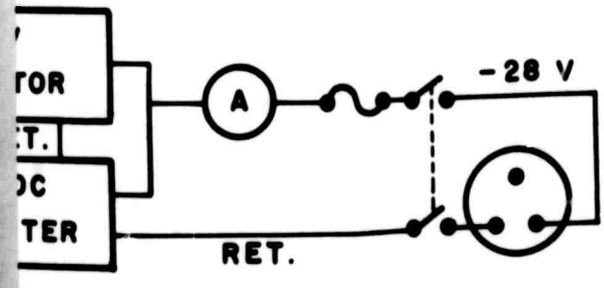

MIC RECEIVING STATION

FIGURE 3

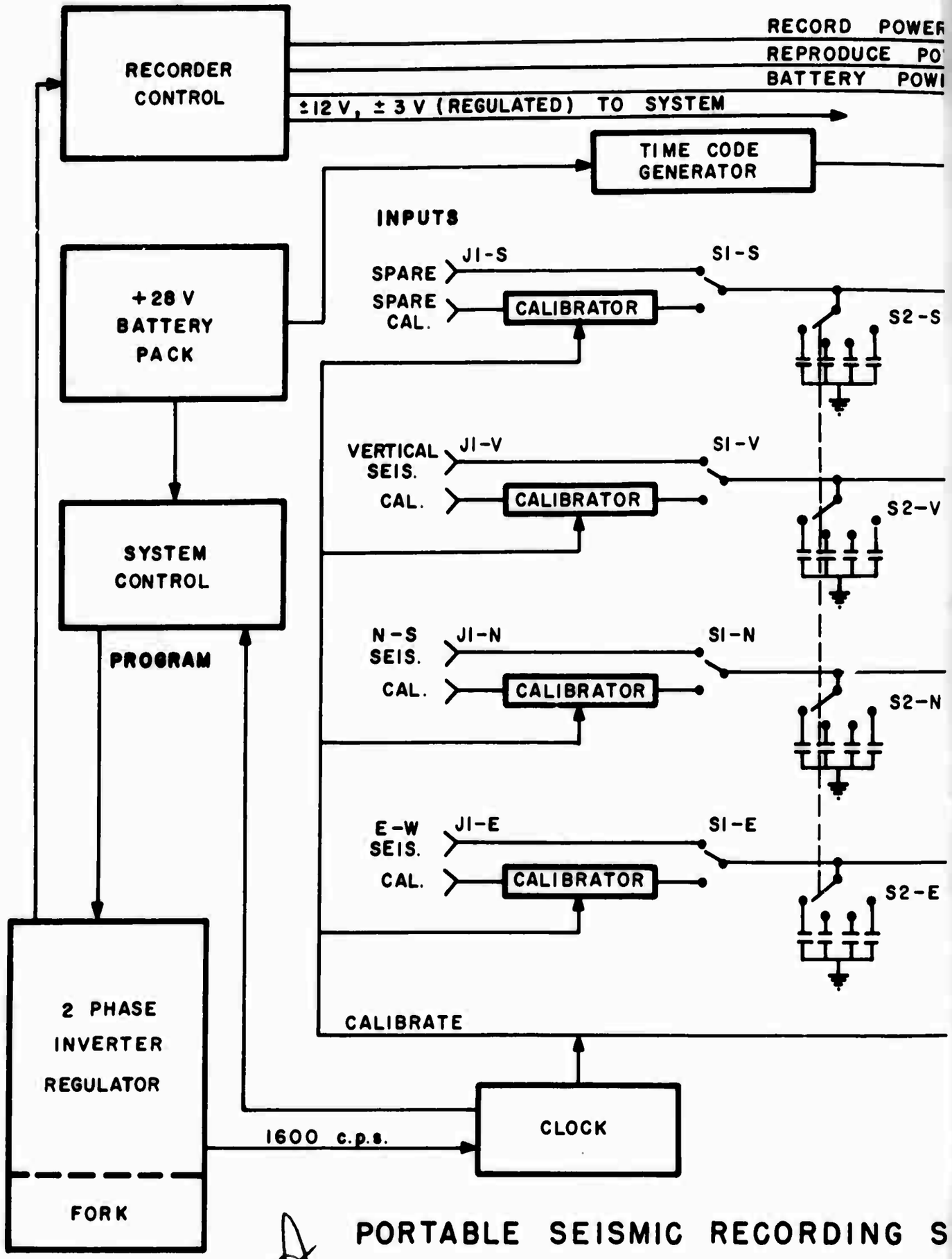

PORTABLE SEISMIC RECORDING S

FIGURE 4

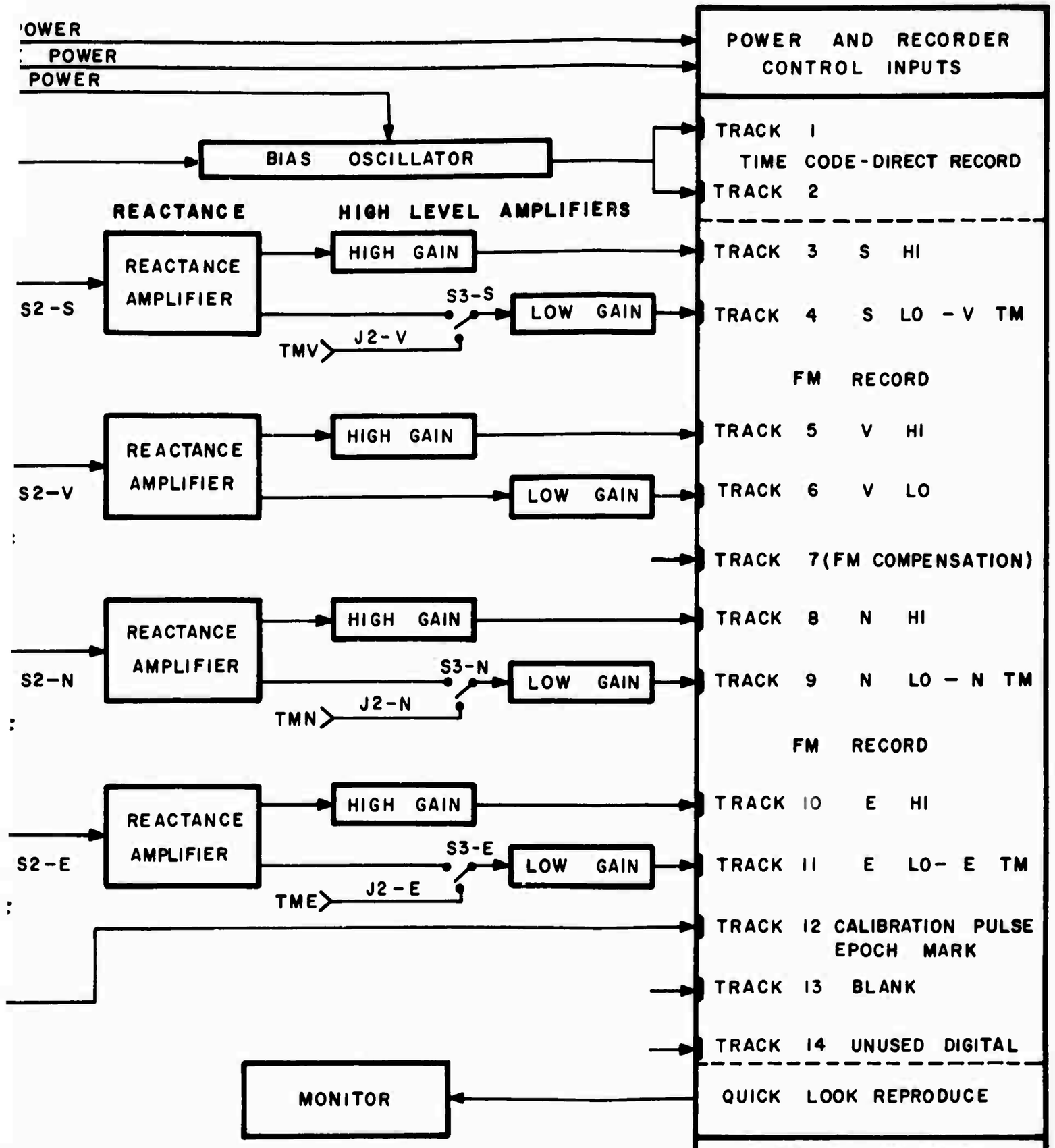

NG SYSTEM - RECORDER PACKAGE

GURE 4

B

BLANK PAGE

3.C Recorder - Receiver Package Interconnection

The J2 - S3 combination is used to permit the recording of signals from the telemetry packages. S3 is actually three switches so that each input channel must be separately switched in with all S3 down. All the parametric amplifiers of the recording package are connected to both sections of the dual gain amplifiers. With the S3 up, the low gain sections of the spare, the east-west, and the north-south channels are disconnected from their associated parametric amplifiers and are connected through J2 to the discriminators of the receiving packages. If just one or two of the S3 are up, then just those corresponding telemetry channels are switched into the recorder. The J2 - S3 combination does not affect the vertical channel of the receiver package. Figure 5 shows a block diagram of the amplifier section of the recording package. Table 1 shows the channel designation in the recording package.

4. Extension of Low Frequency Response

The low frequency response of the portable seismic detection system has been extended to record microseisms. The controlling element for the low frequency response is the feedback

TABLE I

LAR Channel #		Designation
1	Time code - odd tracks	TC1
2	Time code - even tracks	TC2
3	Master unit - spare channel - Hi gain	XMH
4	Master unit - spare channel - Lo gain	XML
	Slave unit - Vertical channel - Hi gain	ZS
5	Master unit - Vertical channel - Hi gain	ZMH
6	Master unit - Vertical channel - Lo gain	ZML
7	Compensation tract	CT
8	Master unit - North-South - Hi gain	NMH
9	Master unit - North-South - Lo gain	NML
	Slave unit - North-South - Hi gain	NS
10	Master unit - East-West - Hi gain	EMH
11	Master unit - East-West - Lo gain	EML
	Slave unit - East-West - Hi gain	ES
12	Master unit - Cal pulse Epoch	CM
13	Not used	
14	Not used	

BLOCK DIAGRAM, AMPLIFIER SECTION OF RECORDER PACKAGE.

FIGURE 5

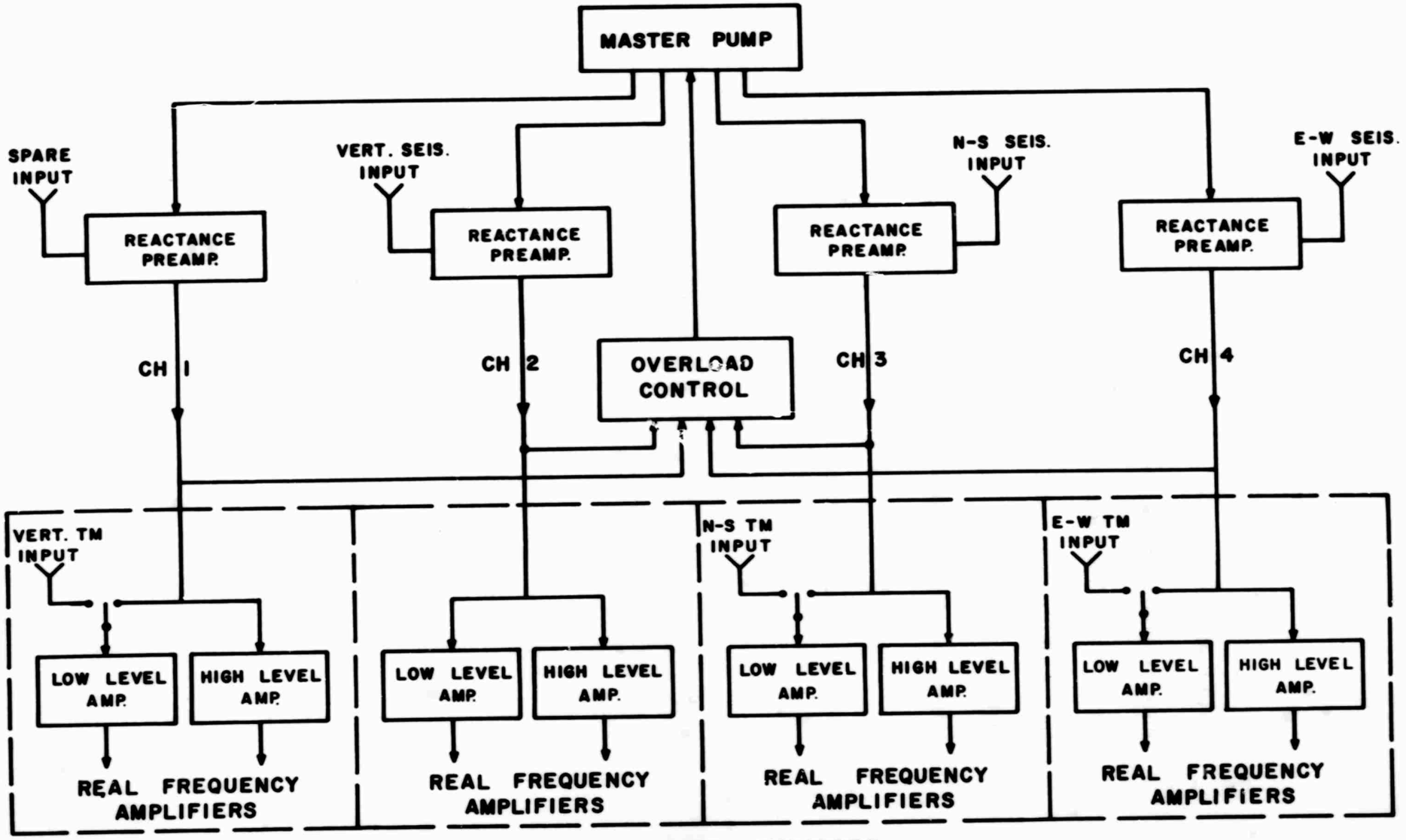

controlled real frequency amplifier. Modification of the feedback network produced the desired response extension. The modifications are shown schematically in Figure 6. In the low level amplifier the capacitors C_5 and C_{10} were shorted. In the high level amplifier, capacitors C_3, C_6 and C_8 were changed to 330 μ farads. Capacitors C_1, C_{11} and C_{12} were increased by 22 microfarads. No changes were necessary in feedback resistor network. The new response is compared to the old response in Figure 7.

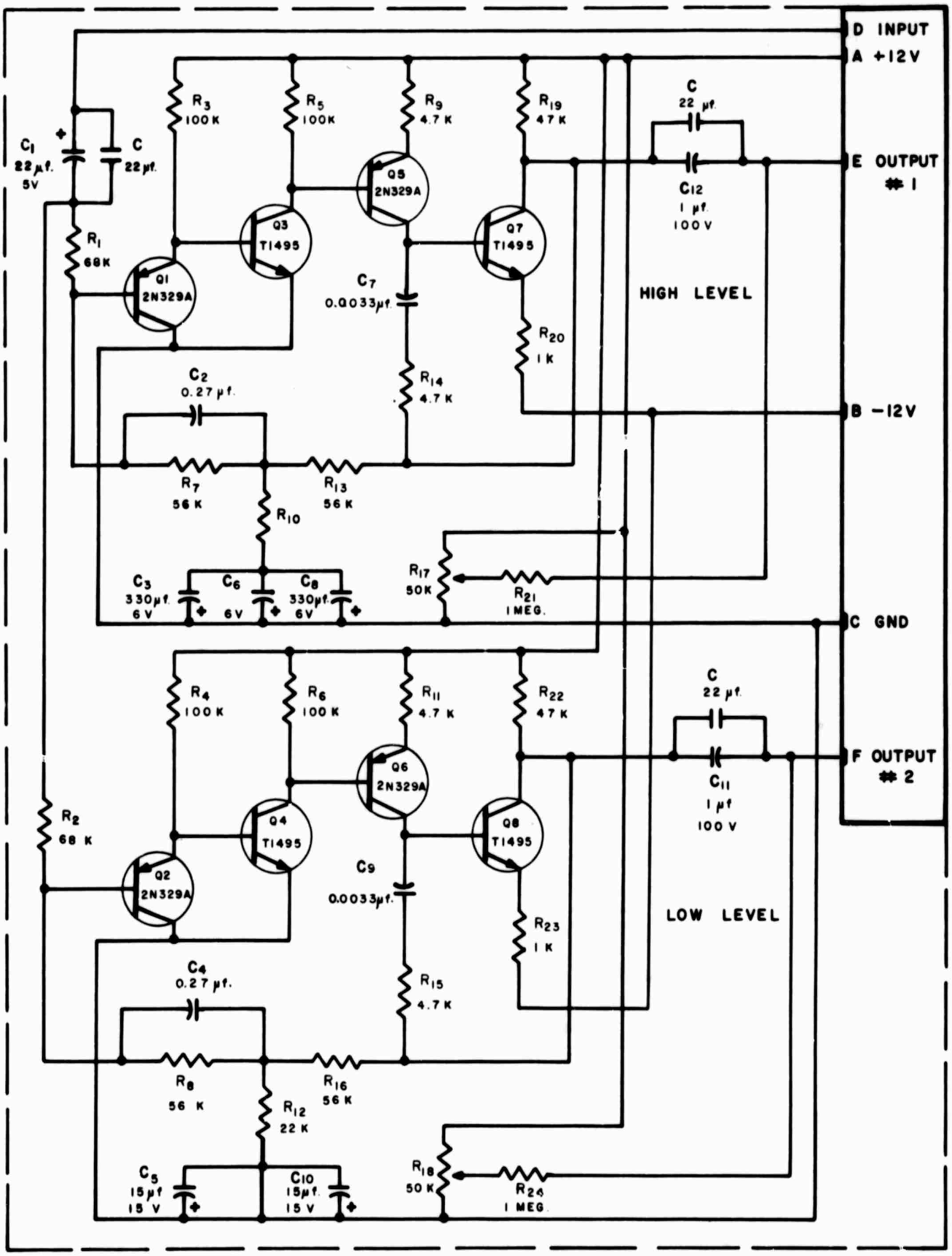

DUAL CHANNEL HIGH LEVEL AMPLIFIER

FIGURE 6

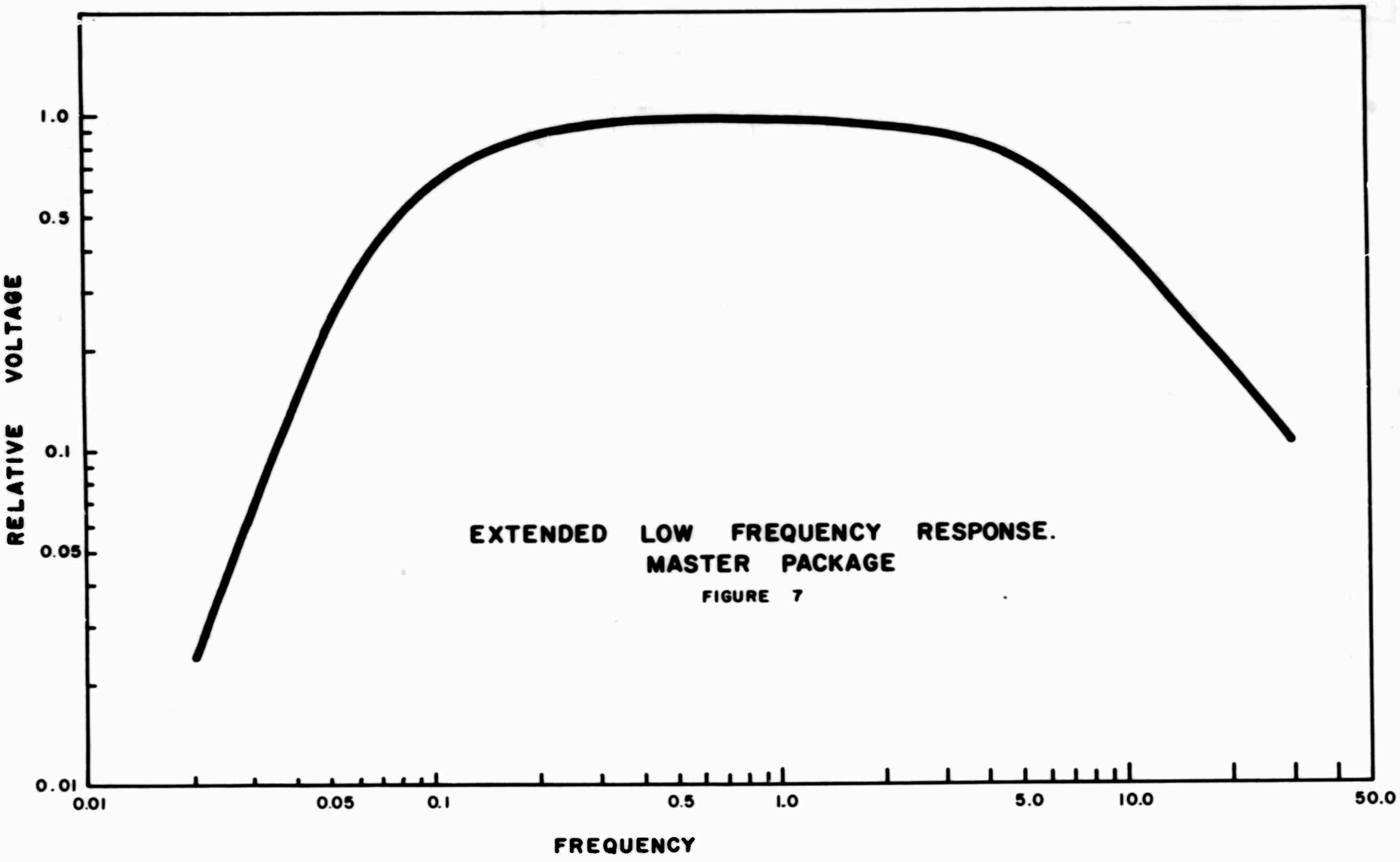

EXTENDED LOW FREQUENCY RESPONSE.
MASTER PACKAGE

FIGURE 7

CHAPTER II

PORTABLE SEISMIC DETECTION SYSTEM TESTS

1. Package Testing

Extensive tests were performed on the portable seismic detection system before the low frequency response was extended and before the capacitor shunts were added. The results of these tests are detailed in this section. The unmodified amplitude and phase responses are presented to exemplify the similarity of responses between packages and to demonstrate the type of results to be expected from testing of this kind. The new amplitude and phase responses have not yet been measured.

The characteristics of the telemetry and recording packages that were measured are the following:

A. In band noise

B. Dynamic range

C. Amplitude response

D. Phase shift

II.1.A In band noise

The in band noise was measured with the input terminated in:

1. A locked seismometer

2. A resistance equal to the seismometer s characteristic resistance (5K ohms)

The maximum noise output was measured to be 24 millivolts. This corresponds to an input noise of approximately 0.5 millimicrons of ground motion.

II. 1.B Dynamic Range

The dynamic range was determined from the following formula:

$$\text{dynamic range (db)} = 20 \log_{10} \frac{\text{maximum non-distorting input}}{\text{equivalent noise input}}$$

The maximum non-distorting input was determined by measuring the input amplitude of a one hertz sine wave that falls just short of producing visible distortion in the output of the recording package's final amplifier stage. The dynamic range of the entire (telemetry and recording packages) system as measured by this method is 48db.

II. 1.C. Amplitude and Phase Responses

The amplitude and phase responses were measured with a sine wave generator and an oscilloscope. The amplitude response was measured by varying the frequency of a constant

amplitude sinusoid input over the range 0.3 hertz to 15 hertz. The output was measured with an oscilloscope at the final stage amplifier in the portable seismic recorder. The output amplitude has been normalized to the amplitude at 1 hertz. The average amplitude response for all channels and all packages is shown in Figure 8. Table 2 shows the percentage variation from the mean of the amplitude response for each channel.

The phase characteristic was determined by measuring the major and minor axes of the Lissajous figure formed on an oscilloscope by using the input to the portable packages as the y trace and the output from the final amplifier section of the portable packages as the x trace.

The average phase diagram for all channels and all packages is shown in Figure 9. Table 3 lists the measured phase angles. Figure 10 shows the Nyquist plot of the average phase and amplitude responses. The accuracy of the measurements are no better than five per cent.

2. Seismometer Testing

This section describes the results of tests performed on the EV17 seismometers. It also describes an alternative testing

TABLE 2

f	Z	%	N	%	E	%
.3	.364	-1.8%	.361	-2.7%	.388	+4.6%
.5	.697	+0.4%	.702	+1.1%	.685	-1.3%
.7	.863	-1.9%	.886	+0.8%	.887	+0.9%
1.0	1.0		1.0		1.0	
1.5	1.11	+2.8%	1.08	0%	1.06	-1.9%
2.0	1.10	+0.9%	1.12	+2.8%	1.06	-2.8%
2.5	1.07	+0.5%	1.07	0.5%	1.06	-0.5%
3.0	1.03	- 1%	1.07	+2.9%	1.05	+ 1%
4.0	.962	-0.1%	.960	-0.3%	.966	+0.3%
5.0	.865	-0.4%	.885	+1.8%	.864	-0.6%
6.0	.773	-1.9%	.793	+0.6%	.797	+1.1%
7.0	.692	-1.1%	.725	+3.6%	.701	0.1%
8.0	.629	-1.1%	.643	+1.1%	.637	0.1%
9.0	.543	- 1%	.569	+3.6%	.547	-0.3%
10.0	.468	-3.1%	.490	+1.4%	.491	+1.6%
15.0						

Deviations of average channel amplitude response from average system response.

TABLE 3

		Z			N			E	
		1	2	3	1	2	3	1	2	3
0.3	-165°	-162		-164	-168		-163	-166		-166
0.4		-129		-129						
0.5	-94°	-106	-81	-103	-98	-81	-98	-98	-81	-98
0.6		-74		-82						
0.7	-69°	-64	-68	-72	-67		-72	-72		-69
0.8	-58°	-55	-59	-62		-54			-58	
0.9		-44	-49	-47						
1.0	-38°	-37	-39	-39	-37	-37	-38	-39	-38	-37
1.5	-5°	-3.6		-5.8	-5		-5.8	-5.8		-4.9
2.0	+17°	+18	+16	+15		18			18	
2.5	+35°	+36		+38	+34		+36	+33		+35
3.0	+51°	+49	+49	+50		+52			+52	
4.0	+75°	+82	+72	+74	74		74	74		77
5.0	+106°	+110	+102	+108		+106			+105	
6.0	+129°	+133	+126	+127	128		132	126		132
7.0	+150°	+157	+149	+148		+143			+155	
8.0	+172°	+180	+168	+168	+171		+174	+171		+174
9.0		+200	+187	+187						
10.0	+214°	+222	+209	+207	+213	+216	+213	+211	+221	+217
15.0	+232°	+224		+246	+231		+233	+233		+226

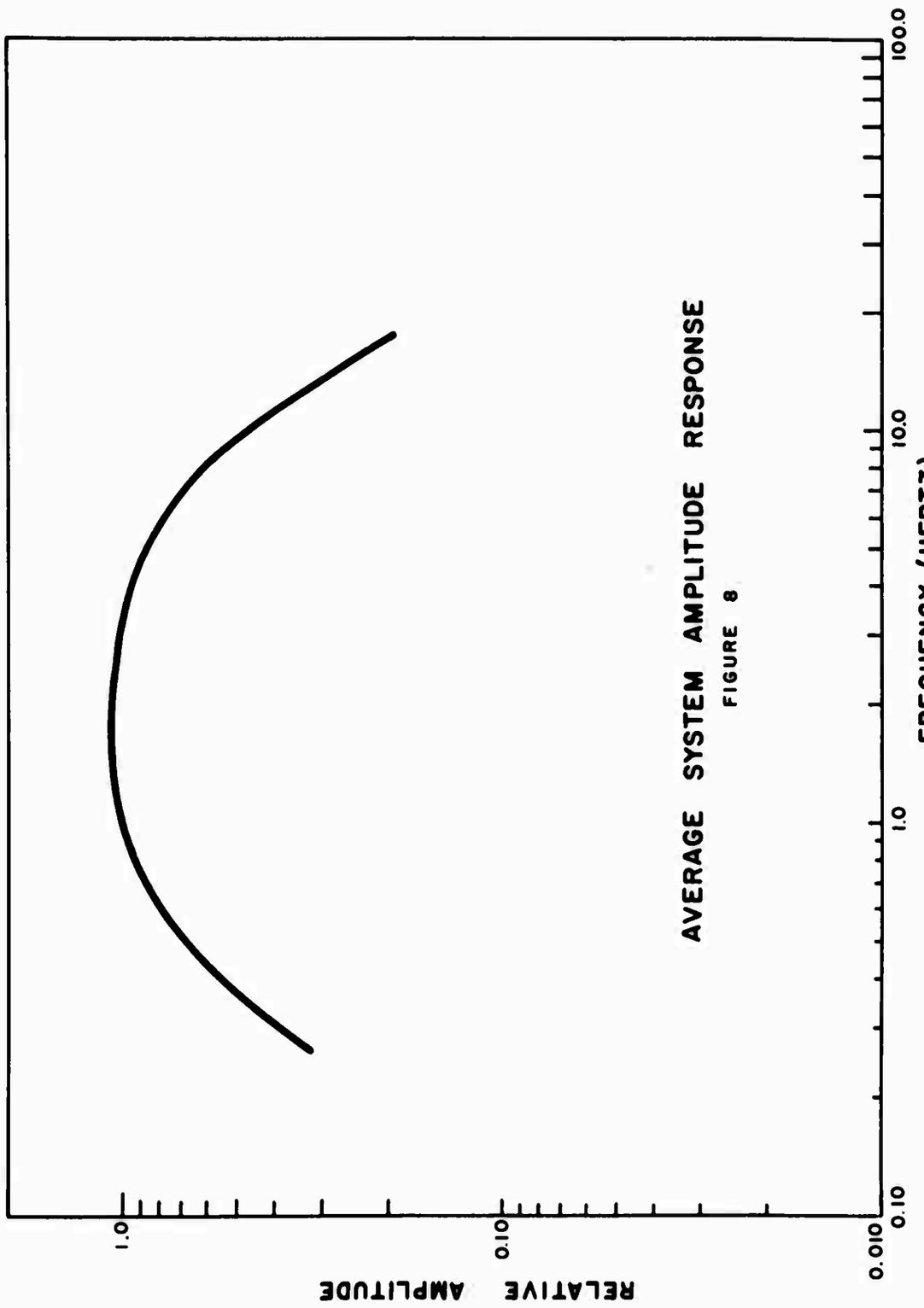

AVERAGE SYSTEM AMPLITUDE RESPONSE

FIGURE 8

26.

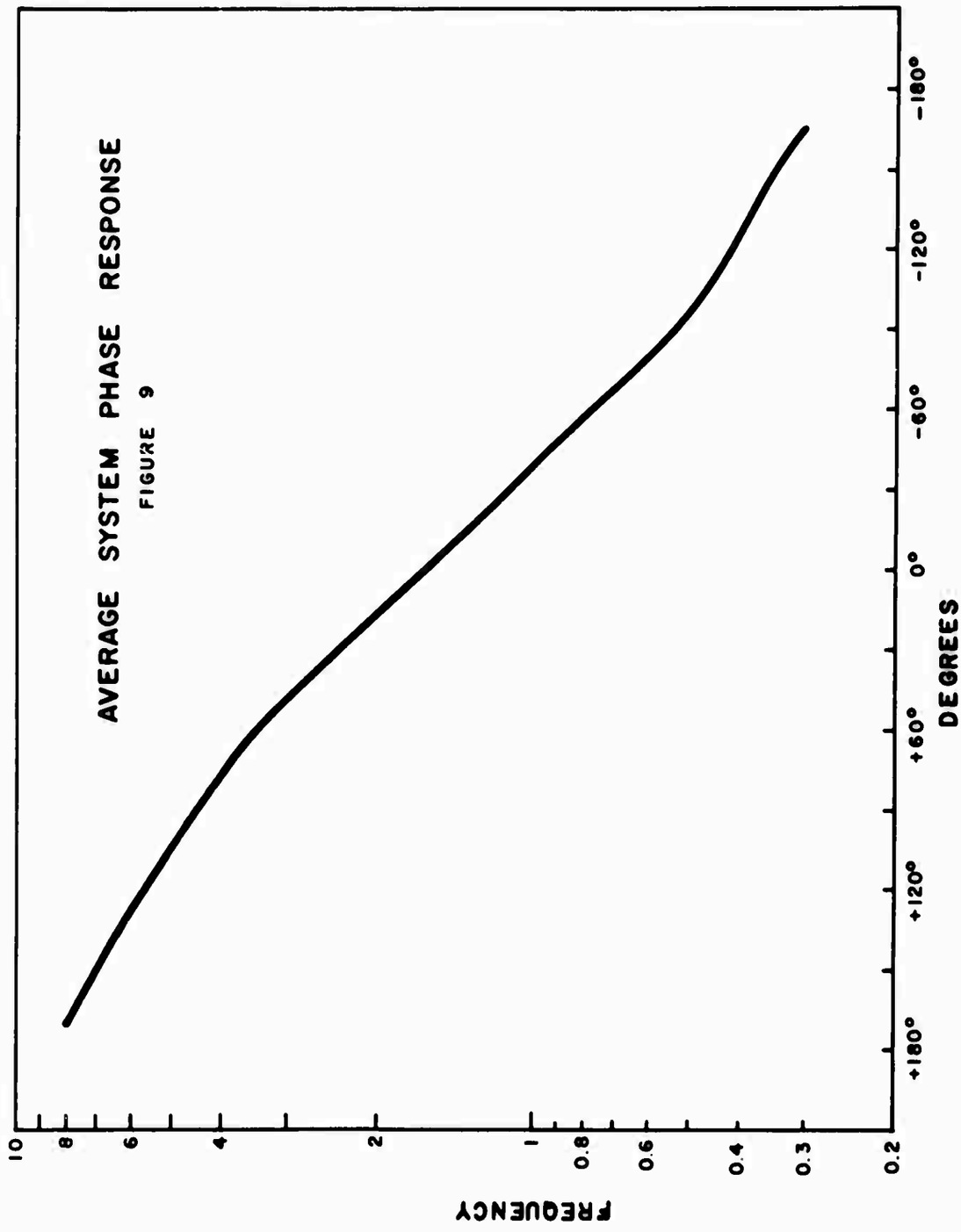
AVERAGE SYSTEM PHASE RESPONSE
FIGURE 9
FREQUENCY
10
8
6
4
2
1
0.8
0.6
0.4
0.3
0.2
+180°
+120°
+60°
0°
-60°
-120°
-180°
DEGREES

27.

AVERAGE NYQUIST - ALL CHANNELS

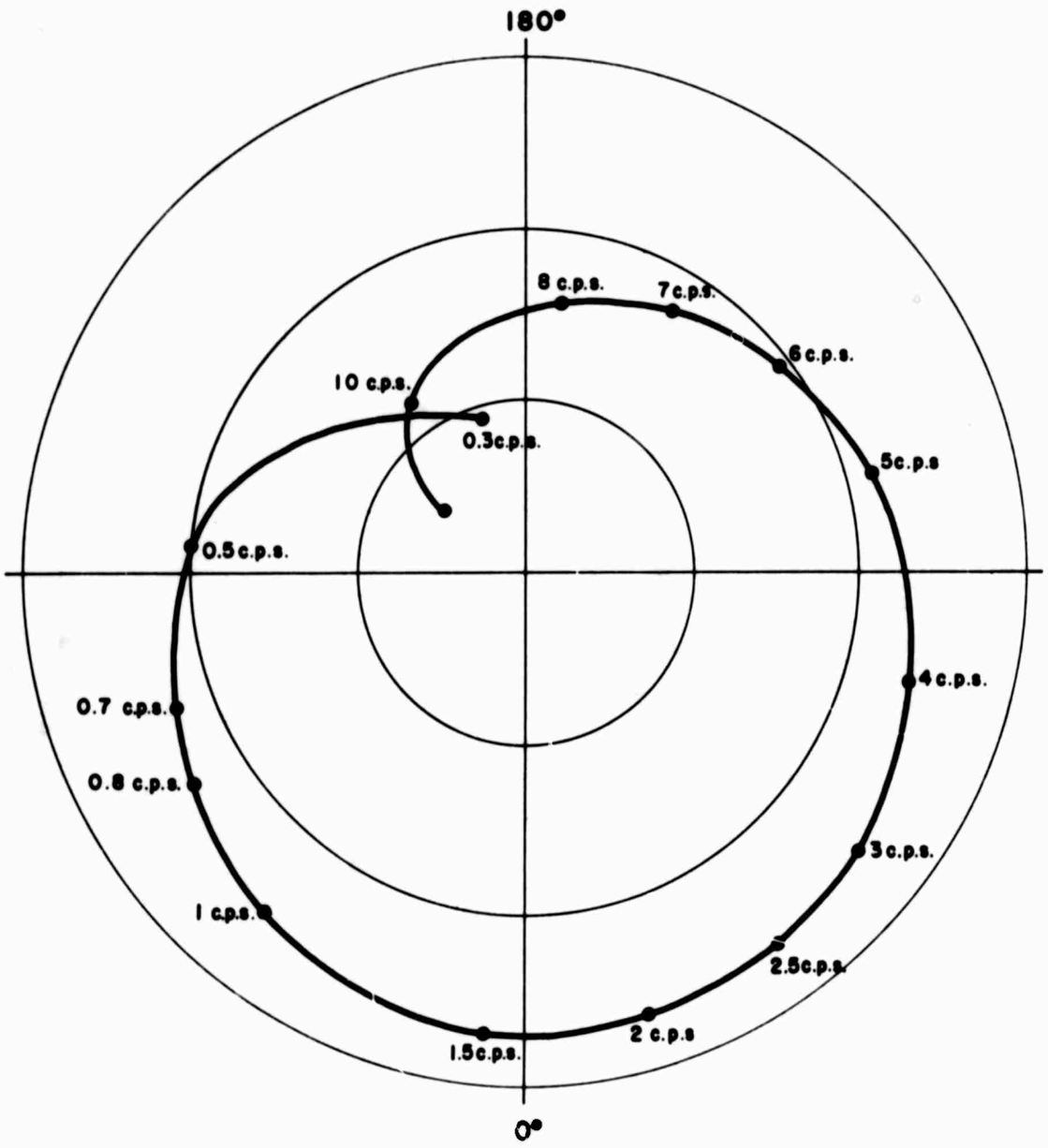

FIGURE 10

procedure for determining the response characteristics of a seismometer with a calibration coil.

The following characteristics of the EV17 seismometers were determined:

A. Motor constants

B. Resonant frequency and variations of resonant frequency due to tilt and temperature

C. Frequency response and location of parasities

D. Linear range

II. 2.A. Motor Constants

The motor constants of the vertical seismometers were determined by both the weight lift and the weight displacement method. The motor constants of the horizontal seismometers were determined only by the weight lift method. The average motor constant was found to be $10.28 \pm .03$ newtons/ampere. A scatter diagram of the measured motor constants is shown in Figure 11.

II. 2.B. Resonant Frequency

The resonant frequency of the EV17 seismometers was determined by using the seismometer sense coil as an element in a resonant circuit and then tuning an oscillator to determine

SCATTER DIAGRAM
SEISMOMETER FREE PERIOD AND MOTOR CONSTANT

FIGURE 11

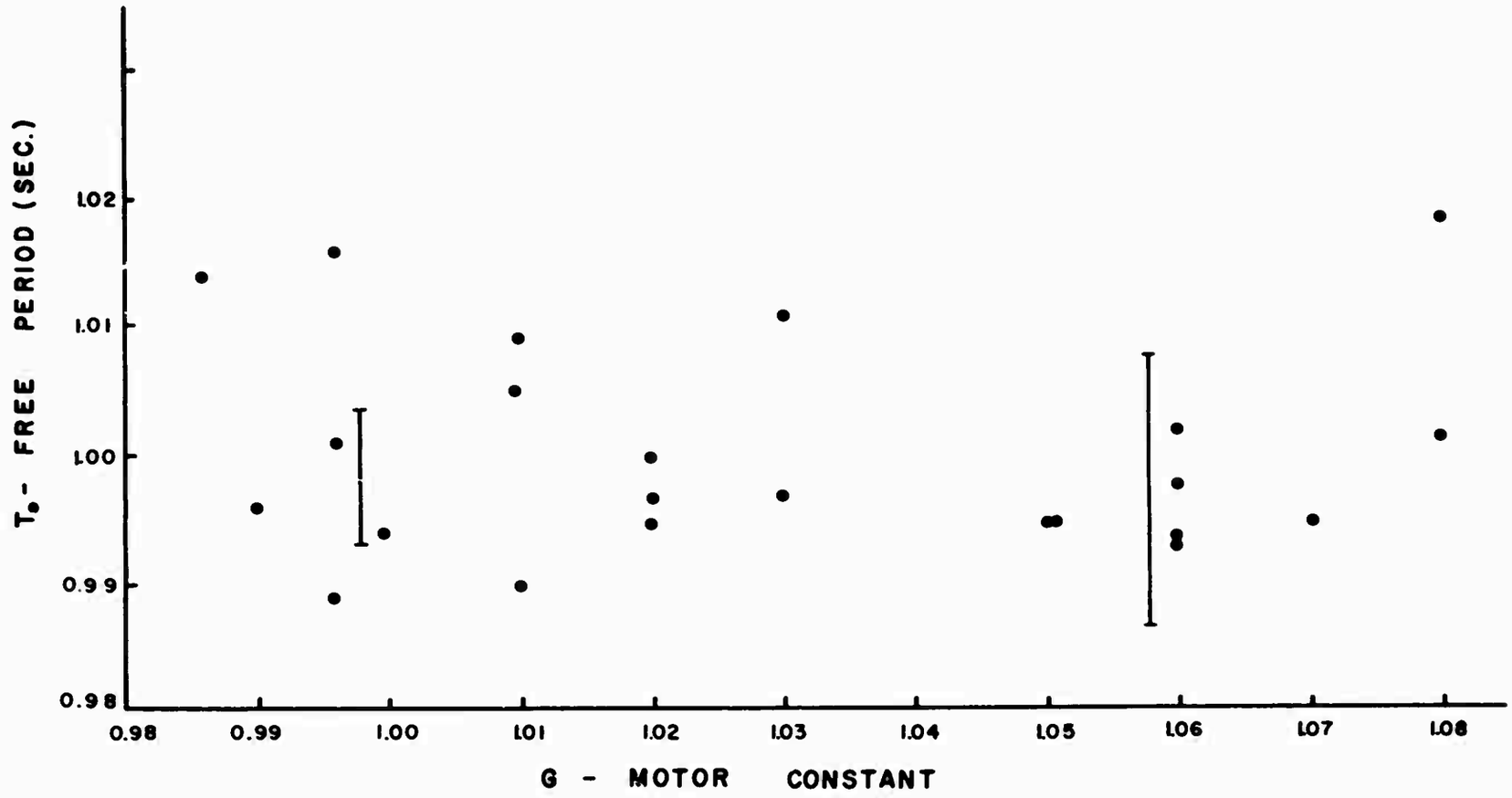

30.

resonance. The variations in natural frequency due to tilts of up to two degrees was also determined by this method. The back of the seismometer was defined as the pivot end. Left and right was defined as the observer's left and right when looking along the seismometer from back to front.

The average natural period was found to be 1.000 ± 0.007 seconds/hertz. The average natural period for the vertical seismometers was 1.001 ± 0.009 seconds/hertz. The average natural period for the horizontal seismometers was 0.999 ± 0.007 seconds/hr. A scatter diagram for natural period is shown in Figure 11.

Left and right tilt produced neglible change in the natural period of the vertical seismometers. Left and right tilt in the horizontal seismometers and front to back tilts in both vertical and horizontal seismometers produced as much as a 7% change from one tilt extreme to the other tilt extreme. Plots of natural period versus tilt for the horizontal and the vertical seismometers are shown in Figures 12 and 13.

II. 2. C. Frequency Response and Location of Parasitics

Frequency response of the EV17 seismometers was

LEFT - RIGHT TILT TEST

FIGURE 12

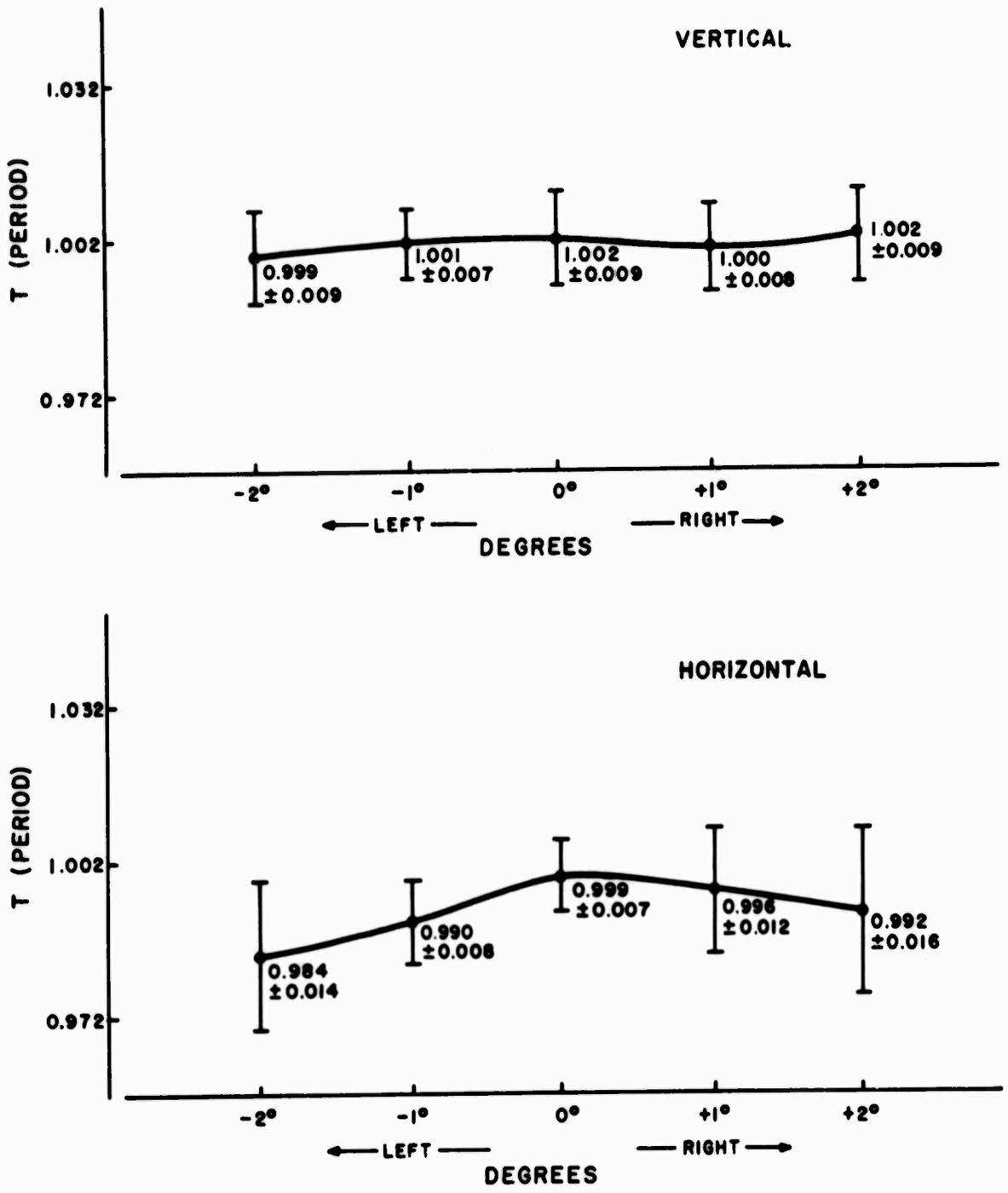

FORWARD - BACKWARD TILT TEST

FIGURE 13

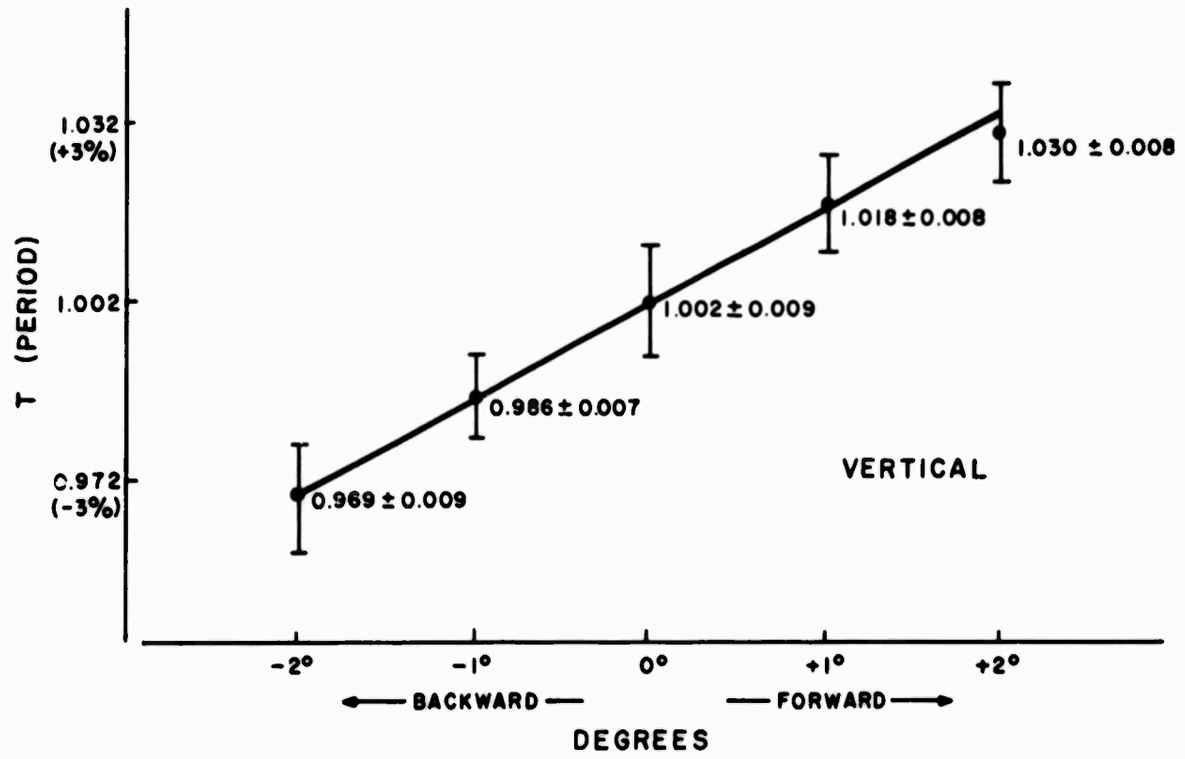

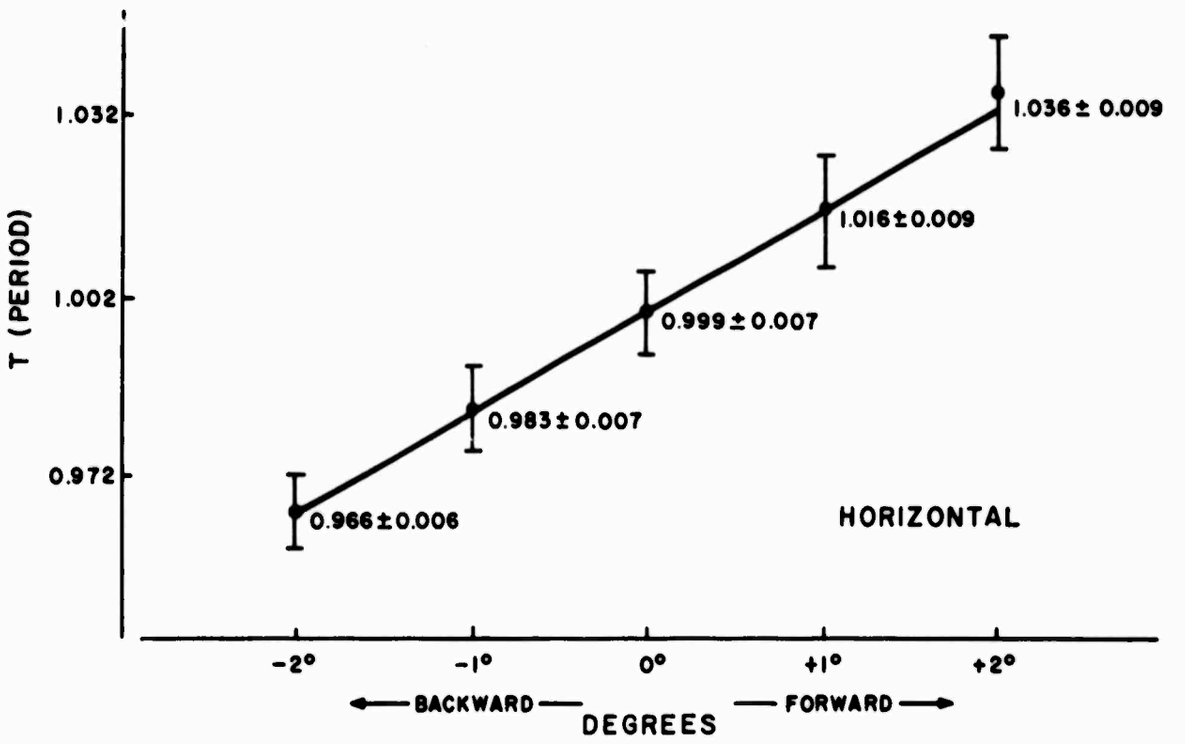

determined by driving the seismometer with a constant amplitude variable frequency sinusoid. The frequency response test was conducted with the seismometer free and with the seismometer locked. The response test indicated a transformer action between the calibration coil and the seismometer coil that became significant above 3 hertz. The average frequency responses for the horizontal seismometers is shown in Figure 14. Curve 2 refers to three seismometers (T1N, T3E, and T2N) which have a response that is about 1% greater than the other horizontal seismometers. Figure 15 depicts the average response for the vertical seismometers. Note that both sets of seismometers have a notch at about 12.5 hertz and significant response above 20 hertz. The response above 20 hertz is due to the transformer action. This is easily seen from the fact that the response above 20hz is the same for both the free and the clamped test. The notch at 12.5 hz is due to the interaction between the transformer action and the normal response of the seismometer. The response curves in Figures 14 and 15 refer to the seismometers alone.

D. Linear Range

The linear operating range of the EV17 seismometers

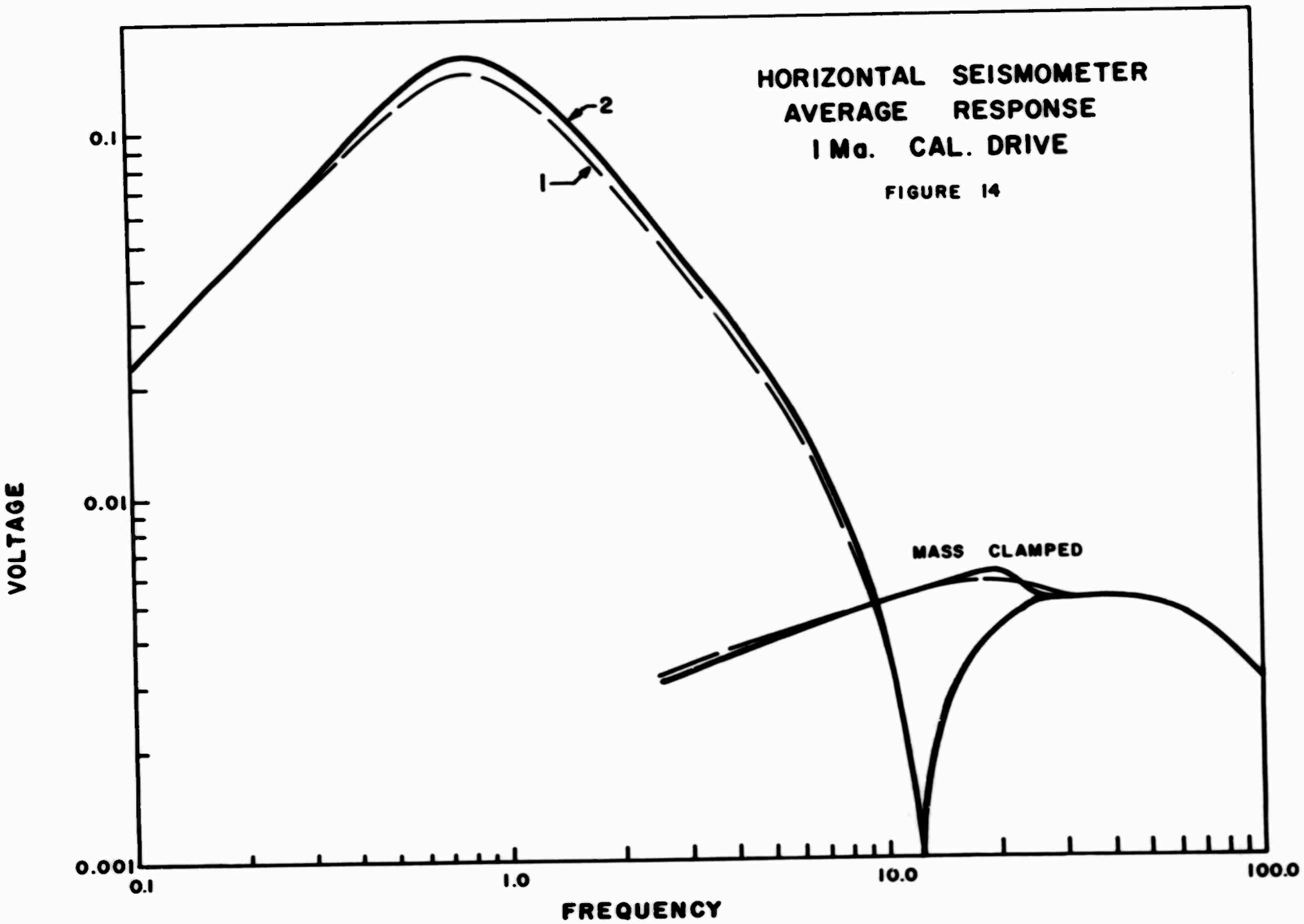
HORIZONTAL SEISMOMETER
AVERAGE RESPONSE
1 Ma. CAL. DRIVE
FIGURE 14
2
1
MASS CLAMPED
VOLTAGE
0.1
0.01
0.001
0.1
1.0
10.0
100.0
FREQUENCY

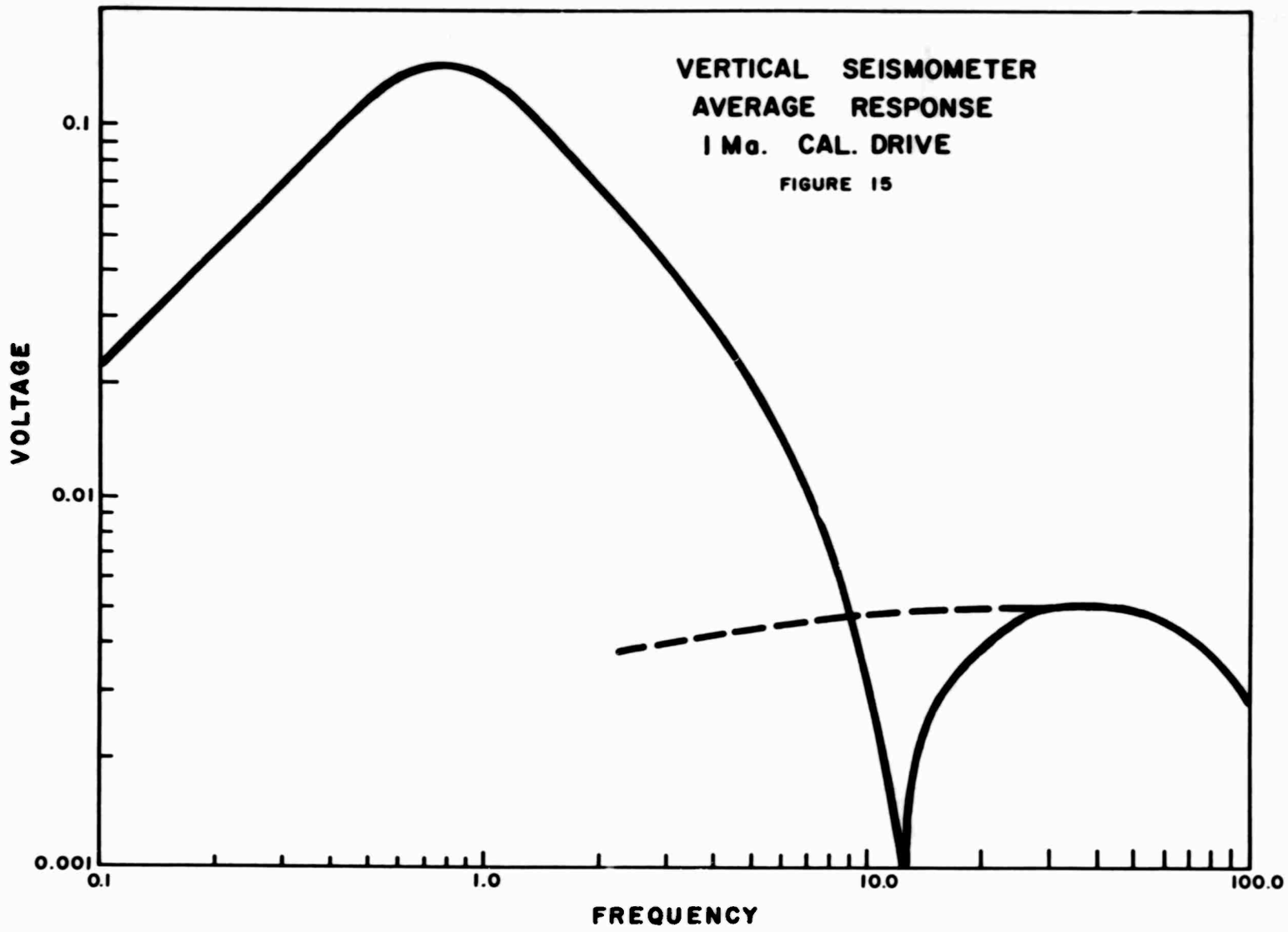
VERTICAL SEISMOMETER
AVERAGE RESPONSE
1 Ma. CAL. DRIVE
FIGURE 15
VOLTAGE
0.1
0.01
0.001
0.1
1.0
10.0
100.0
FREQUENCY

36.

was measured by applying known currents to the calibration coil and observing the resultant displacement with a telescope. This method was not entirely satisfactory since it did not give accurate measurements in the region 10-20 microns displacement and gave no measurements below 10 microns. A least squares analysis showed the data could be fit in the 20 to 200 micron displacement region by a straight line having a slope of 95.7 microns per milliampere.

II. 3. Seismometer Testing

Determining the response characteristic of a seismometer is a particularization of the general problem of determing the dynamic characteristics of a constant parameter linear system. It is appropriate at this point to review the definition of a constant parameter linear system.

A system has constant parameters if all the fundamental properties of the system are invariant with respect to time. In simple terms, this means that the system will function in the same way tomorrow as it did today. A system is linear if the response characteristic is additive and homogeneous. A system is additive if the output of a sum of inputs

is equal to the sum of the outputs produced by each input separately. A system is homogeneous if the output produced by a constant times an input is equal to the constant times the output produced by the input alone.

If a system is characterized by a function $h(t)$ and the input and output of the system are designated by $x(t)$ and $y(t)$ respectively, then a constant parameter linear system may be mathematically characterized in the following way:

Constant parameter: $h(t) = h(t+\Delta t)$ for all Δt

Linear: $a \sum X_L(t) \longrightarrow a \sum y_L(t)$

If the operating environment and the range of inputs are suitably restricted, the assumption that a physical system is a constant parameter linear system is valid. The operating restrictions vary from system to system but are generally known from manufacturer's specifications.

The dynamic characteristics for a constant parameter linear system can be descrived by a weighting function, $h(\tau)$. The weighting function is defined as the output of the system at any time to a unit impulse applied a time before. A constant

parameter linear system can also be characterized by a transfer function H(P), which is defined as the Laplace transform of $h(\tau)$. That is,

$$H(p) = \int_{-\infty}^{+\infty} h(\tau)\, e^{-p\tau}\, d\tau$$

where $p = a+ib$.

The value of the weighting function as a description of a system is due to the fact that for any arbitrary input x(t), the output of the system may be specified as a convolution of the input with the weighting function.

$$(1) \qquad y(t) = \int_{-\infty}^{+\infty} h(\tau)\; x(t-\tau)\, d\tau = h(t)*x(t)$$

for a system to be physically realizable the output cannot reflect future inputs. This restricts $h(\tau)$ to be zero if τ is less than zero.

A third method of characterizing a constant parameter linear system is in terms of its frequency response function, which is defined as the Fourier transformer of $h(\tau)$. That is,

$$H(f) = \int_{0}^{\infty} h(\tau)\, e^{-i\omega\tau}\, d\tau$$

Note that the lower limit of integration is zero rather than minus infinity since $h(\tau) = 0$ for $\tau < 0$. The frequency response function is simply a special case of the transfer function where, in the exponent $p = a+ib$, $a = 0$ and $b = 2\pi f$.

An important relationship for the frequency response function of constant parameter linear systems is obtained by taking the Fourier transform of the convolution integral relating input to output. Letting $X(f)$ be the Fourier transform of the input $x(t)$ and $Y(f)$ be the Fourier transform of the resulting output, it follows that

$$(2) \quad Y(f) = H(f)\, X(f)$$

Hence, in terms of the frequency response function for a system and the Fourier transforms for the input and the output, the convolution integral reduces to a simple algebraic expression.

The frequency response function is generally a complex valued quantity which may be conveniently written in complex polar notation as

$$H(f) = |H(f)|^{-i\phi(f)}$$

The absolute value $H(f)$ is called the system gain factor and the associated phase angle $\phi(f)$ is called the system

phase factor.

It is clear that the frequency response function of a constant parameter linear system can be written as

$$H(f) = \frac{Y(f)}{X(f)}$$

where Y(f) is the measured response and X(f) is the transform of the known input. For the special case where X(f) = 1 for all frequency. (x(t) is a delta function), then H(f) = Y(f). In this case H(f) is known as the impulse response of the system. In practice, X(t) can be considered a delta function if its transform is reasonable flat across the frequency band of interest.

Seismometer Testing Procedure:

The test procedure is illustrated schematically in Figure 16. The Bay State 601 is a fixed program statistical analyzer which is used as the controller in these tests.

In the Dynamic Average A&B mode the 601 will, besides separately averaging the inputs to memories A and B, generate a 6 microsecond pulse at intervals selected by the sample rate and the setting in the analysis period thumbwheels. This output pulse is amplified to fifty volts and widened to twenty

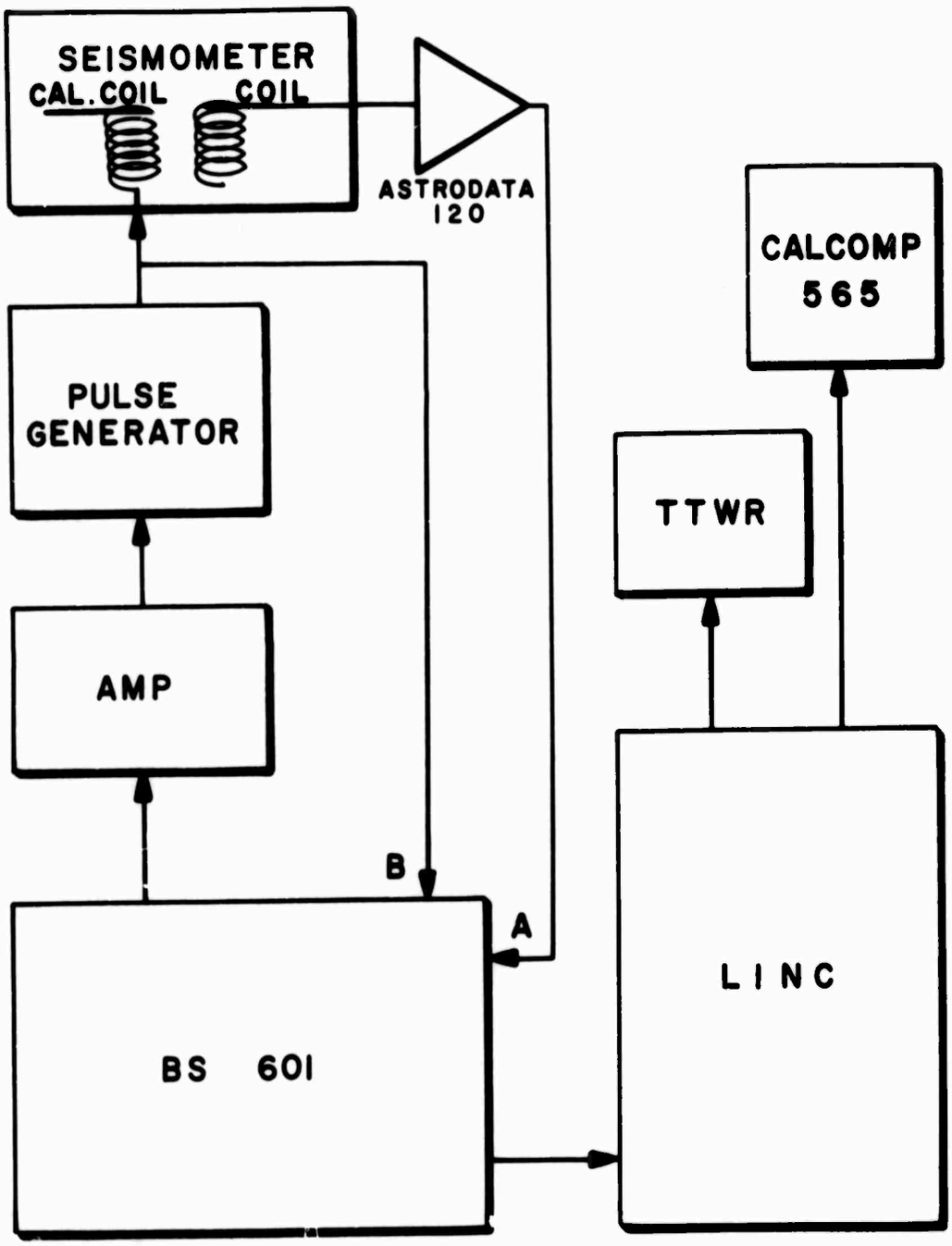

SEISMOMETER TEST SYSTEM

FIGURE -16

milliseconds by means of a pulse generator. Amplification is done to minimize line pickup. The twenty millisecond width was convenient. The pulse is then simultaneously transmitted to the pier room and entered into the 601 as channel B. At the test pier this input pulse is divided down through a voltage divider and is used as a calibration current for the calibration coil in the seismometer. An astrodata Nanovolt amplifier, model 201, is used to amplify the seismometer response. The amplified seismometer response is returned to the Data Analysis Lab where it is used as the input to channel A in the 601.

The pulses are repeated several times to minimize the effect of background noise. A digital counter is used to count the number of calibration pulses. When a sufficient number of calibration pulses have been sent to insure a good signal-to-noise ratio, the calibration pulse and the seismometer response are then transferred to the μ - LINC, where they are individually Fourier transformed. Using the real and imaginary parts of the transforms, the system gain factor and phase angle can easily be computed

A word about the repetition rate of the calibration pulse is in order. It must be remembered that the seismometer is

responding to normal seismic noise during the period of test. To minimize the effect of this background noise, the repetition rate of the calibration pulse should be chosen to insure that the background noise is uncorrelated. In particular, since the normal microseismic background peaks near six seconds, the separation between calibration pulses should be significantly longer than six seconds. By insuring incoherence between the background noise and the calibration wavelet, the signal-to-noise ratio will be improved by the square root of the number of calibration wavelets employed.

An example of the application of this seismometer testing procedure is found in the 1967 Annual Report of this contract.

CHAPTER III

DATA ANALYSIS LABORATORY

Introduction

Work in the data analysis laboratory has been directed primarily toward the writing and implementation of programs that will facilitate the reduction of data taken with the portable seismic detection system. Some engineering work to upgrade the capabilities of the data analysis facility has also been performed.

The programming work involves the construction of a program system, tilted DISPATCH, that will direct and monitor the data reduction process. The engineering work has involved the fabrication of interface equipment for the computer. The two items constructed are a digital counter-computer interface and a computer-digital plotter interface.

III. 1. DISPATCH System

Dispatch is a reserved block system designed to control the processing of data that has been recorded by the portable seismic detection system. There are four distinct sections to the system. The first section controls the digitization and transfer of analog data. The second section corrects the digitized

data. The third section obtains a few basic statistics of the corrected data. The fourth section obtains the auto and cross spectra of the corrected data.

III. 1.A. Digitization and Transfer of Data

The data to be digitized is selected by the operator from a playout of the analog data. Once the events have been selected, they may be digitized by the computer. The only information required by the LINC is the minute before the desired start time and the duration of the event of interest. The LINC, using the time code recorded with the data (IRIG C format), will digitize three channels of data at a real time sampling rate of 100 samples per second per channel. The channel assignation for the portable seismic packages is listed in Table 1. The digitized data will be stored on Datamec digital tape in IBM compatible format.

The Datamec digital tape is regarded as the main storage area. Unprocessed data is held in working files prior to processing. Processed data is held in library files. A working file starts with an odd parity four word (12 bits per word) record containing the unit number, the package number, and the start time.

The identification record is followed by N data records, where N is the number of kept seconds. Each data record consists of three hundred odd parity (decimal) words corresponding to one second's worth of data from each of three channels. The three channels of data are interleaved in the format 1, 2, 3 ... 1, 2, 3. The end of file is marked by two even parity octal seventeens.

A library file is similar to a working file. The identification record has thirty octal odd parity words that enumerate the processing that has been performed on the data. The data files are six hundred odd parity words in length. Figure 17 shows a schematic layout of the working and the library files. Both working file tapes and library file tapes start with an end of file mark.

Figure 17

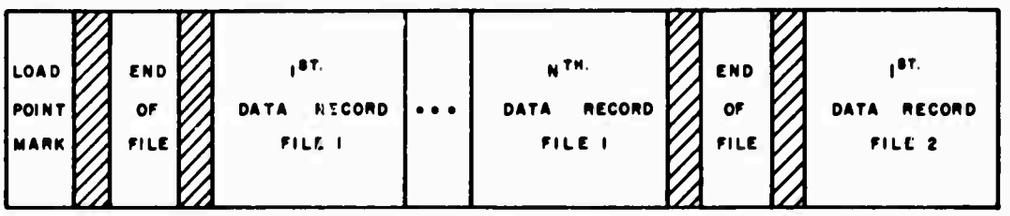

For processing, data is transferred from Datamec tape to LINC tape since all processing of data is performed on the LINC. The amount of data to be transferred is specified in terms of time. Up to four minutes of data may be stored on one LINC tape. The start storage time is determined by advancing the Datamec to the desired file and then displaying the desired file on the LINC's oscilloscope. The time associated with each display is shown with the data. When the desired start time is displayed the transfer process may be initiated by the operator. The prime feature of this process is that the data to be transferred must be transferred as a titled group. Up to ten titled groups may be stored on one LINC tape. After the data transfer has been effected, the LINC resumes its data display at the first second following the last record of transferred data.

The digitization and transfer section also permits the transfer of titled data groups and of titled correlations and histograms among the various LINC units. Processed data groups may be transferred to a library file on the Datamec.

III. 1.B. Data Correction

All correction processes are performed on data

stored on the LINC tape units. Tape units 1, 4 and 5 have been preassigned as data units. Tape unit 0 has been preassigned as the program unit.

The correction processes may be applied to data in the following three ways:

1. To a particular titled group on a particular data unit.
2. To a particular title group on all three data units.
3. To all titled groups on all three data units.

To facilitate processing, each data tape carries a data index which is stored in Block 0 and lists each data entry on the tape. There may be up to ten decimal entries in an index. Figure 18a shows a sample data index. Note that an identifier consisting of 5757 s occupies the first ten octal locations of the data index and that each unused space in the index contains a 5757. Each data group is allocated thirty octal words in the index. Figure 18b demonstrates a sample entry. A key feature of the entry is the section that maintains the status of the data. Each time an operation is performed on the data the status section is consulted. If the operation has not been previously done the

FIGURE 18

18a Sample Data Index

Location	Description
0-7	Index Identifier
10-37	Entry 1
40-67	Entry 2
70-117	Entry 3
120-147	Entry 4
150-177	Entry 5
200-227	Entry 6
230-257	Entry 7
260-307	Entry 8
310-337	Entry 9
340-367	Entry 10
370-377	Unused

18b Sample Data Index Entry

0	EX	
1	AM	Title Entry
2	PL	
3	E1	
4	0001	Starting Block
5	0103	Start Hours
6	0407	Start Minutes
7	0000	Start Seconds
10	0235	End Block
11	0103	Package and first half of test day
12	0408	End minutes
13	0200	End Seconds
14	0101	Last half of test day and channel
15	YE	Zero Flag
16	YE	Filter Flag
17	0034	Standard deviation
20	0007	Maximum Value
21	5757	2 dimensional histogram, not done indicator
22	YE	Auto-correlation flag
23	5757	Cross correlation, not done indicator
24	YE	Scale flag
25	5757	Rotate, not done flag
26	5757	Unused
27	5757	Unused

appropriate status entry is updated and the operation is performed. If the operation has already been done the operator is asked if he wishes to redo the operation. If he does, the operation is performed; if he does not, the operation is omitted. This feature is included to prevent unintentional modification of the data.

The correction processes that can be performed are the following:

1. Amplitude equalization, or scaling
2. Bias removal, or zeroing
3. Filtration
   A. Low pass
   B. High pass
   C. Band pass
4. Rotation of coordinate axes

DISPATCH assumes that the correction processes will be applied in the sequence specified above. That is, the data will first be scaled and then zeroed. Filtration and rotation can be performed only on data that has been zeroed.

The sequencing of the operations can be attributed to both the ideosyncrasies of individual programs and to the data tape format. For example, scaling before zeroing is recommended because the zeroing program computes the standard deviation of

the data and it is advantageous to have the standard deviation refer to the amplitude equalized trace. The data tape format is involved because the storage of corrected data is a function of the particular correction that has been applied.

The data storage area on a data tape lies between and includes blocks 1 to 765. Every 200 decimal words (2 seconds of data) are assigned a four block storage area. For example, if 10 seconds of data are kept, uncorrected data is stored in blocks 1, 5, 11, 15 and 21. The next data group entry would start at block 25. The structure of each four block storage area is shown in Figure 19. The first block contains unprocessed data or data that has been scaled. The contents

Figure 19

1	2	3	4
UNPROCESSED OR SCALED DATA	HISTOGRAMS OR EMPTY	FILTERED AND/OR ROTATED DATA	ZEROED DATA

of this block are dependent upon the status of the processing. If the second block belongs to one of the first five storage areas of a group it will contain either a one dimensional histogram or

one-fourth of a two-dimensional histogram. If the second block is not a member of one of the first five storage areas it will be empty. The third block will contain scaled and zeroed data that has been either filtered or filtered and rotated. The data in the third block is the data that is correlated. The fourth block will contain data that has been scaled and zeroed.

III. 1.C. Statistics Section

The statistics section will perform the following four operations:

1. Obtain a one-dimensional histogram of scaled and zeroed data.
2. Obtain a two-dimensional histogram of scaled and zeroed data mounted on units 1 and 4.
3. Auto-correlate filtered data.
4. Crosscorrelate filtered data.

All statistics are performed on titled groups of data. The one-dimensional histogram and standard deviation is routinely computed by the zeroing program but may be repeated here. The two-dimensional histogram programs provides an alphabetic teletype output of the conditional probability of B

given A. A is the data on unit 1, B is the data on unit 4. The program assumes that a tape containing the third component of the data group being worked with is on unit 5. Table 4 lists the printout scale used.

The auto-correlation and cross-correlation programs transfer data groups from a specified unit on the LINC to the BS 601 Statistical Analyzer. The correlations are performed on the BS 601. Both auto and cross correlations are set up to give a power spectrum extending from 0 to 12.5 Hz. This requirement means that every data point is used in computing the cross-correlation function while every other data point is used in computing the auto-correlation function.

The correlations, when recalled from the BS 601, are filed on a correlations tape which must be separate from the data tape. Each correlation is assigned a ten octal block storage area on the correlations tape. This storage area size was chosen so as to provide a working area for the Fourier transform programs.

The correlations tape carries its index in blocks 0 and 1. The index identifier for the correlations tape consists of 10 octal 7575's. The identifier is located in the first ten

TABLE 4

*	0-4	W	1280-1394
A	5-9	X	1395-1514
B	10-19	Y	1515-1639
C	20-34	Z	1640-1769
D	35-54		1770
E	55-79		
F	80-119		
G	120-154		
H	155-194		
I	195-239		
J	240-289		
K	290-344		
L	345-404		
M	405-469		
N	470-539		
O	540-614		
P	615-694		
Q	695-779		
R	780-869		
S	870-964		
T	965-1064		
U	1065-1169		
V	1170-1279		

locations of the index. Room for sixty-three decimal index entries has been provided. Each index entry area is ten octal words long. Unused index locations contain 7575. A sample index entry is shown in Figure 20. Note the inclusion of the Bay State output gain and of the Fourier transform scale factor. These numbers are carried to enable the operator to obtain a rapid estimate of the relative sizes of various spectra. To facilitate plotting to scale, the Bay State output gain is carried in the first location of each correlation while the difference between the Bay State output gain and the transform scale value is carried in the first location of each transform.

Figure 20

```
EX
AM          TITLE
PL
E1
0100        BLOCK STORAGE
1000        BAY STATE OUTPUT GAIN
-3          TRANSFORM SCALE FACTOR
7575        BLANK
```

III. 1.D Computation of Auto and Cross Spectra

In its present configuration, DISPATCH will compute only one-sided transforms that have been weighted with a Hanning function. The transform program will, by using the correlation tape index, transform all correlation entries on a tape. Updating of all entries in the index will take place when all transforms have been completed. The total scale value associated with each transform will be computed and stored with each transform as each transform is completed and stored. The block assignation within each ten octal block storage area is shown in Figure 21.

Figure 21

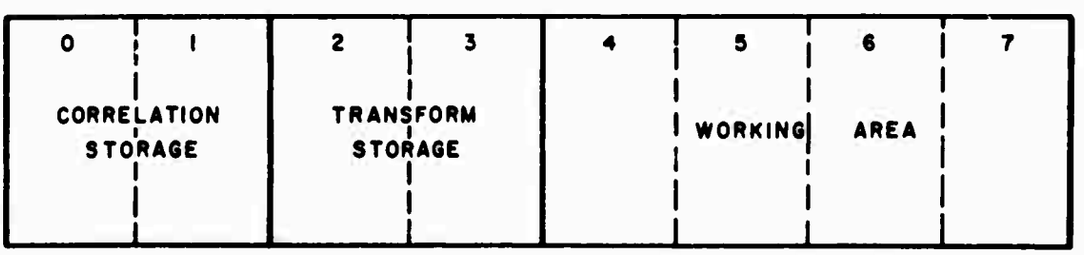

COMPUTER - PLOTTER INTERFACE

The computer-plotter interface is due to Mr. Lee Bacon of the Southwest Graduate Research Center. The interface consists of a Digital Equipment Inverter card (DEC 4102) which has been modified in the following way. The clamping diode color coded as in 003 and the 1.7K resistor in the collector circuit have been removed. The 1.7K load resistor has been replaced with a 470 ohm resistor. With the modifications the circuit works in the following way. Application of a minus three-volt pulse to the base of Q1 drives Q1 into saturation. This causes the collector of Q1 to go from minus fifteen volts to approximately zero volts. This fifteen volt positive going pulse is used to step the Calcomp plotter. Figure 22a shows the original circuit and Figure 22b the modified circuit.

Table 5 shows the computer to plotter connections.

Table 5

Operate Line	Plotter Function
OPR 7	Drum up
OPR 10	Drum down
OPR 11	Carriage right
OPR 12	Carriage left
OPR 13	Pen up
OPR 14	Pen down

INVERTER FOR CALCOMP INTERFACE

FIGURE 22

a) ORIGINAL CIRCUIT

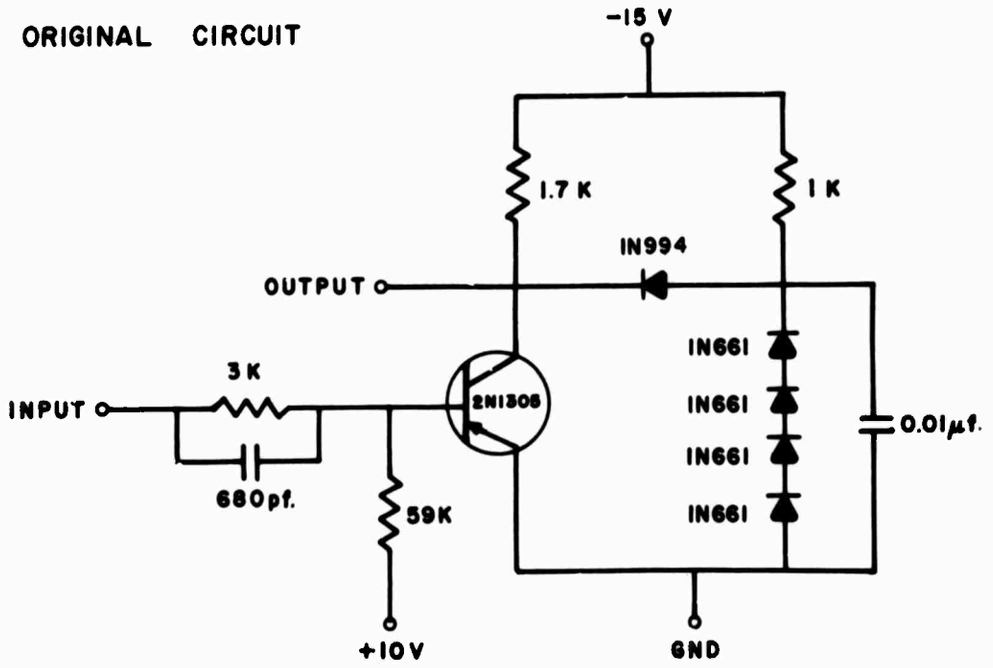

b) MODIFIED CIRCUIT

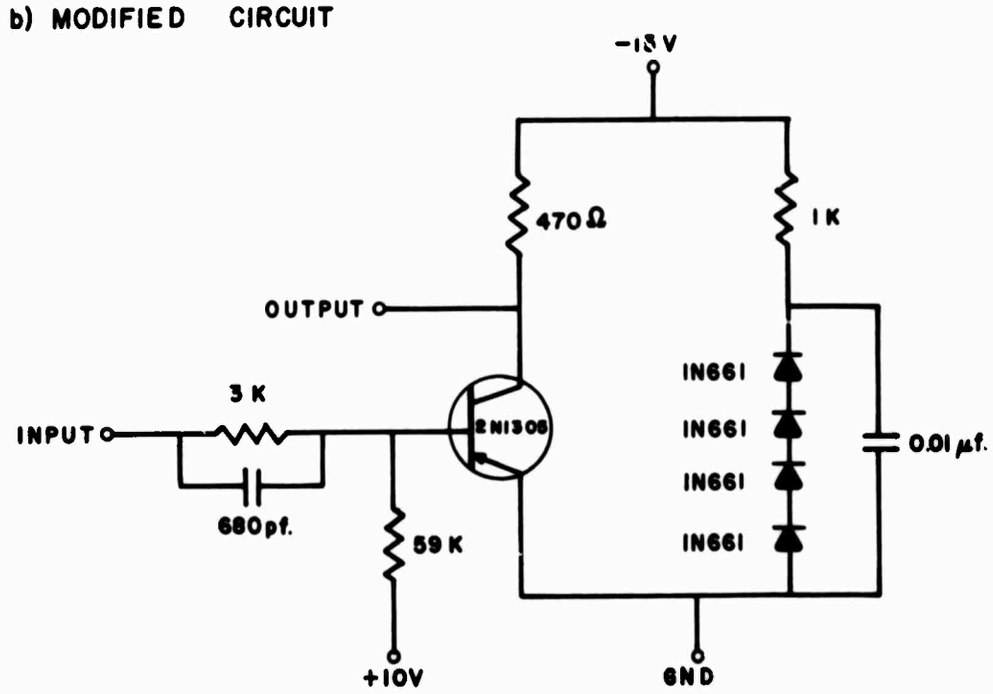

Digital Entry to the LINC (Thomas E. Foley)

The digital entry logic modules were designed to allow the LINC to accept the digital output of Hewlett-Packard's 5000 series electronic counters. The logic levels for these counters are the following:

Logic 0 = -28 volts dc

Logic 1 = - 2 volts dc

These logic levels are supplied through a 100koh ı source impedance. High impedance schmitt trigger circuits using a clamped output voltage between 0 volts dc and -3 volts dc were used to convert the counter BCD to the LINC logic levels of 0 volts and -3 volts. The truth table conversion between the Hewlett-Packard counters and the LINC is given in Table 6.

Table 6

HEWLETT PACKARD		LINC	
Logic		Logic	
0	(-28v)	1	(-3v)
1	(-2v)	0	(0v)

The schematic of the schmitt trigger is shown in Figure 23. Using these schmitt triggers, the LINC may, upon

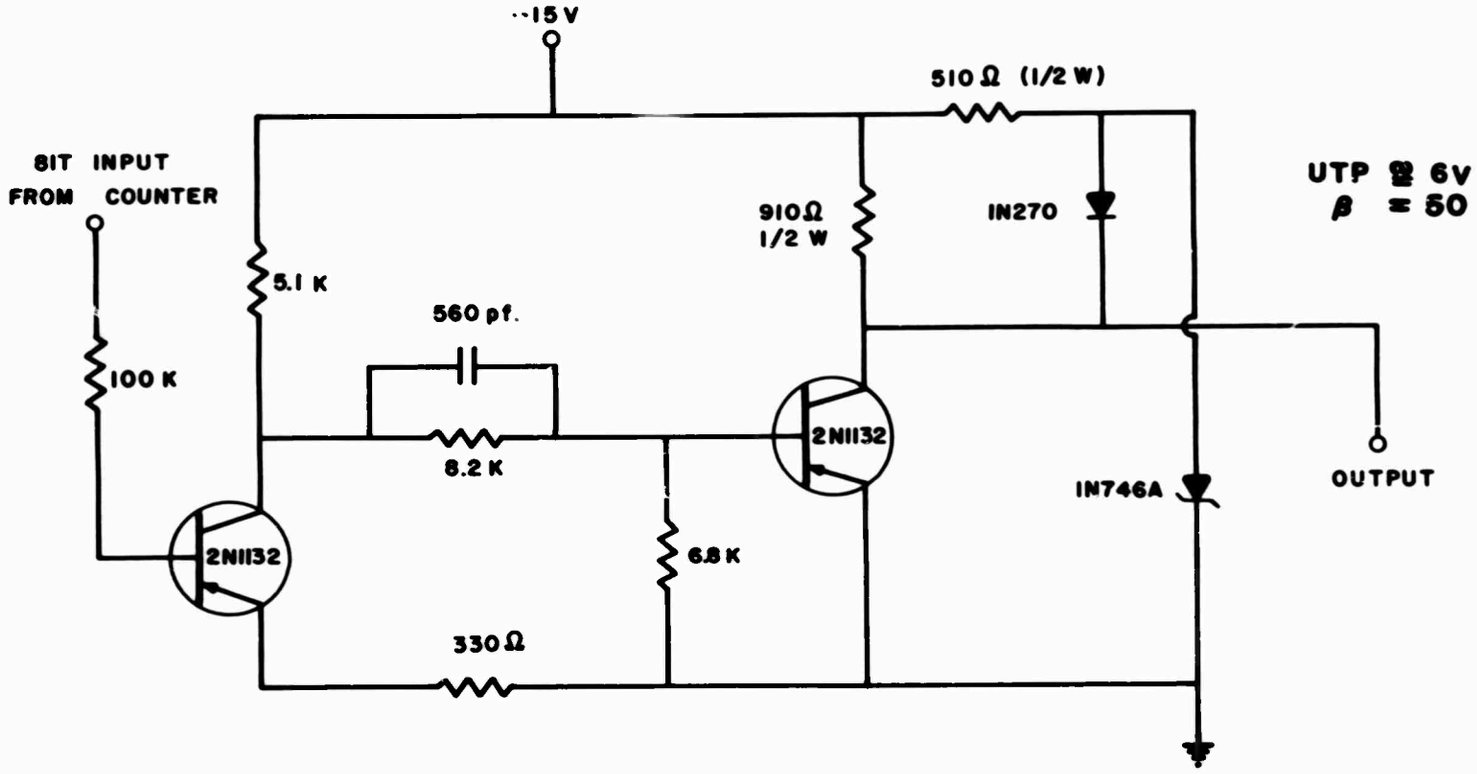

SCHMITT TRIGGER FOR COUNTER

FIGURE 23

61.

command, read up to 4 12 bit digital words into memory. The words are read in one at a time as complemented BCD.

A logic module was constructed which enables the LINC to reset the electronic counter. The LINC will provide, upon command a negative pulse to one of sixteen output command lines. The pulse is 6μ seconds wide and is -3 volts in amplitude. In order to drive the counter reset circuit this negative pulse is widened and applied to a solenoid driver. The pulse from the LINC is widened and applied to the solenoid driver in the following way. The computer pulse is applied to a high input impedance schmitt trigger which provides a -3 volts to 0 volts pulse from a 1 kohm source to a monostable multivibrator. The multivibrator triggers a solenoid driver which drives the reset relay for the counter or counters. A schematic of the schmitt trigger and multivibrator is shown in Figure 24. A block diagram of the system is shown in Figure 25.

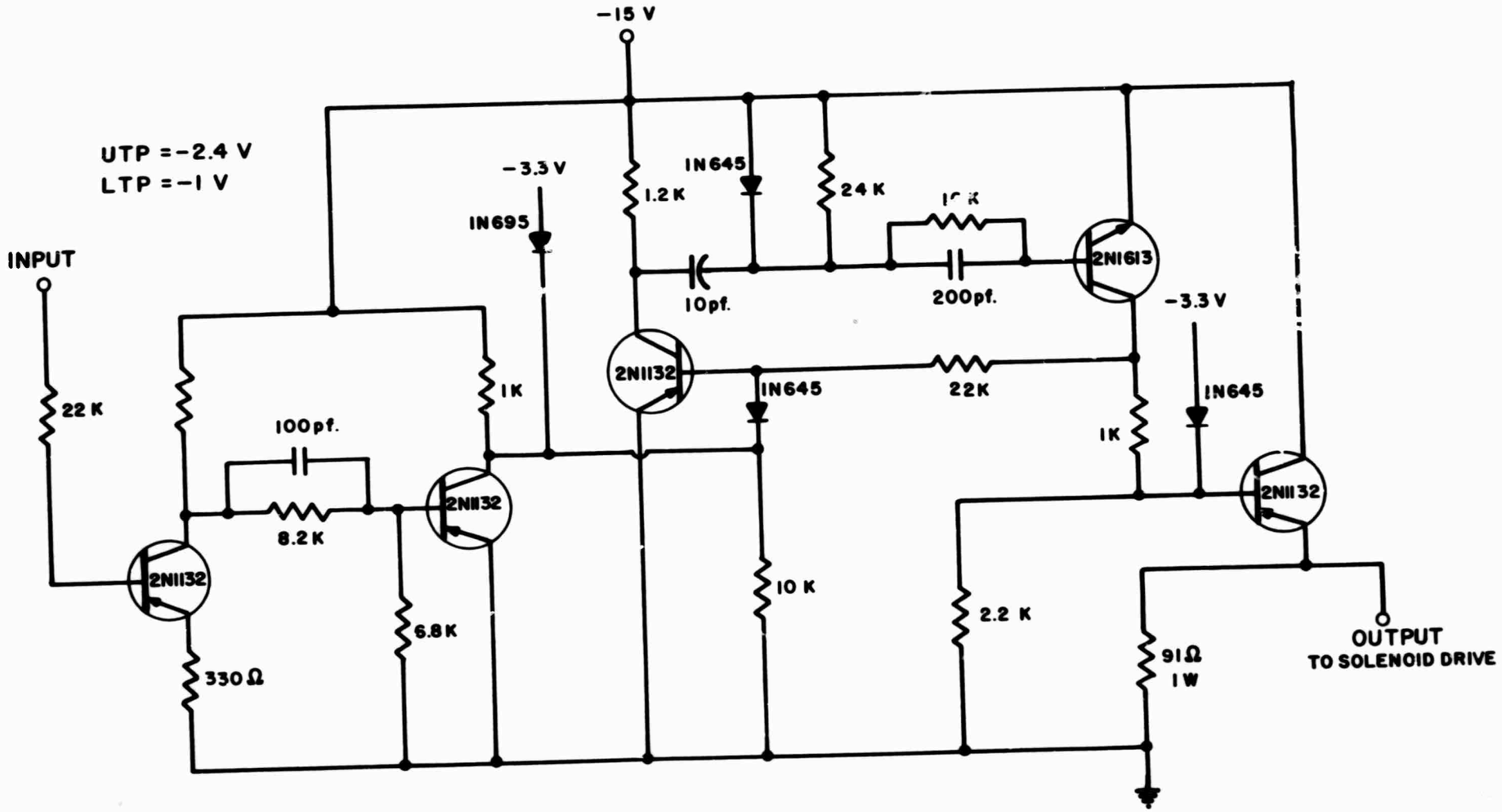

SCHMITT TRIGGER AND MONOSTABLE

FIGURE 24

63.

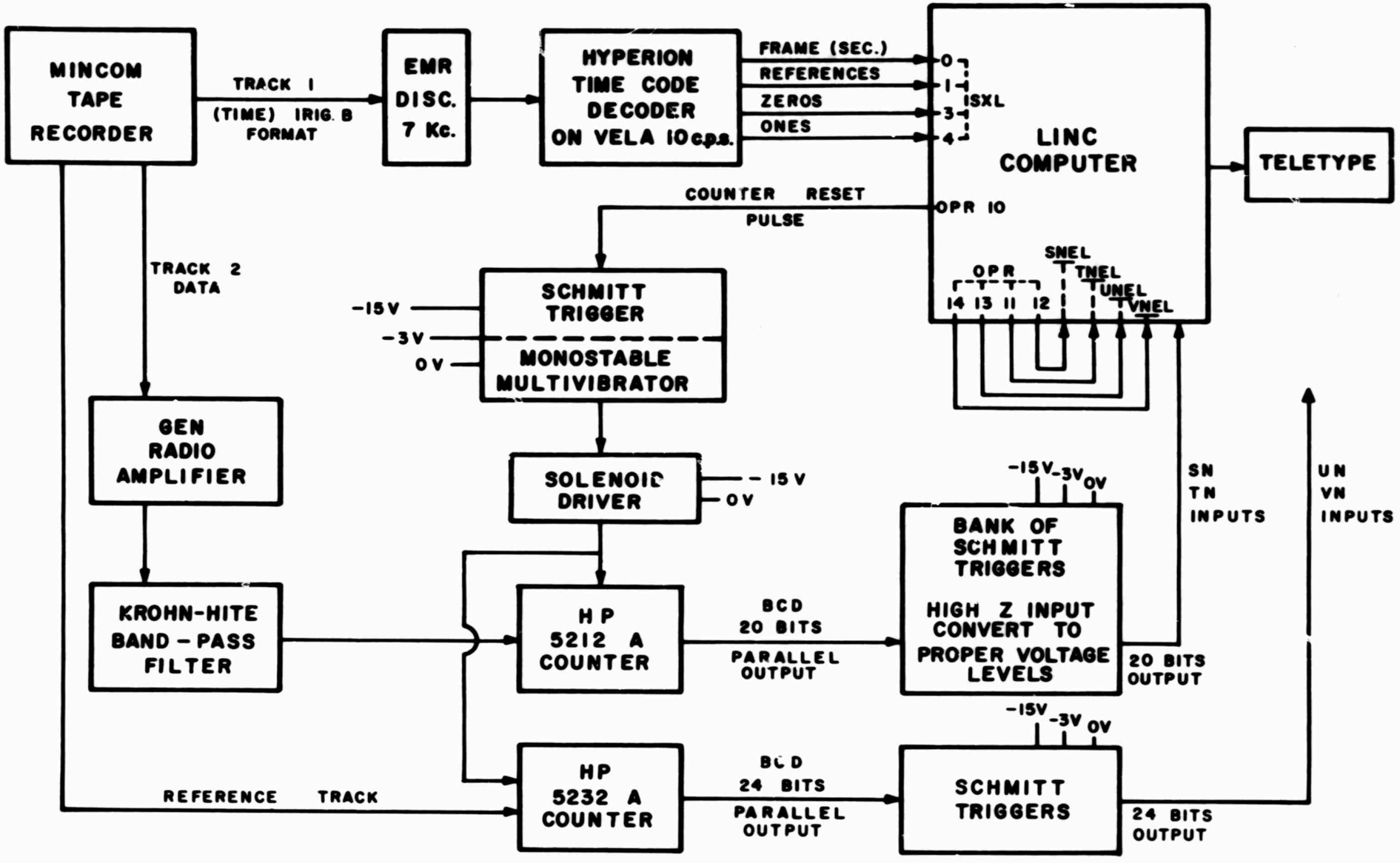

SYSTEM BLOCK DIAGRAM.

FIGURE 25

64.

CHAPTER IV

The Weston Gravimeter and Tiltmeter System

The sensor elements employed in the Weston system were designed to act as time dependent switches. For an understanding of this method of operation consider first the gravimeter element as an example, the operation of the tiltmeters being analogous, and refer to Figure 26. As the force of gravity increases, the mass M will be pulled down tending towards equilibrium with the force developed in the spring system according to Hooke s Law. As soon as photodiode A receives more light from the beam splitter than photodiode B, the electronic circuitry will start delivering pulse energy to coil A. This pulse energy in coil A will drive the mass back towards the zero position. Because the system has very low damping, the zero point will be overshot, the electronics will reverse states and, by applying pulse energy to coil B, will drive the mass down again. Thus the motion of the element will be a continuous oscillation.

In addition to delivering the pulse energy to the servo coils, the electronics also deliver the same pulses to an Atec, Inc. Model 601 Differential Counter. This counter has the ability to count the difference between the number of pulses delivered to the A coil and the B coil. Thus, if gravity has increased, the sensor

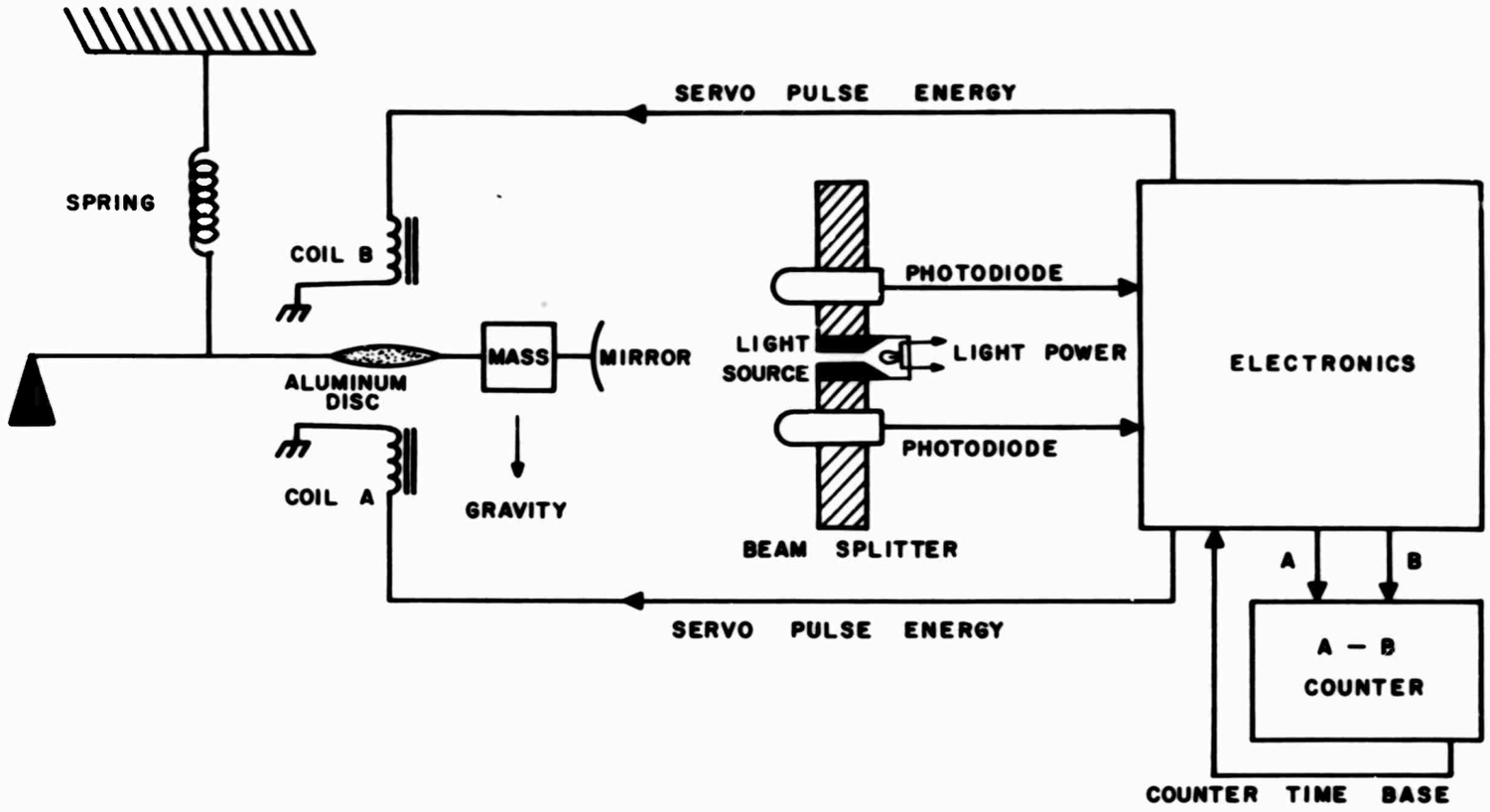

SIGNAL FLOW DIAGRAM DIGITAL SYSTEM

FIGURE 26

element will spend more time on the A side of the zero position than on the B side and the A-B count as registered in the Atec counter will be positive. Similarly, if the gravitational force decreases, the element will spend more time on the B side and the A-B total will be negative. By dividing this time into small increments, i.e. using a high pulse repetition frequency, and by integrating the effect over many oscillations of the element, a high degree of resolution can be obtained. The Atec counter supplies the pulses from its own time base with the selection of 250kHz, 100kHz, or 10kHz and integration intervals of 100, 10, or 2.5 seconds. Assuming a pulse rate of 250kHz and an integration time of 100 seconds, an equivalent voltage dynamic range of 154 db. is obtained, considering that the total can go from $+2.5 \times 10^7$ to -2.5×10^7 counts and assuming that ± 1 count can be resolved and that there is no noise errors generated in the photodiode sensing. Although this figure is the optimum theoretical value, it indicates that the system can provide dynamic range beyond that of any typical analog system.

The tiltmeters work in an entirely analogous way in that if the sensor frame is tilted from the zero position, the element, in tending towards alignment with the local gravity vector, will spend

more time during its oscillations on one side of the zero position than the other. Figure 27, 28, 29 indicate that the gravimeter is of the spring balance type, and the tiltmeters are of the pendulum type, sensitized by using a inverted section to approach instability. Figures 30, 31 show a system timing diagram for two cases.

The tiltmeter elements were partially built for Weston Observatory by Worden Quartz Products, Inc. of Houston, Texas. Subsequent modifications were made at Weston. The gravimeter element was fabricated at Weston using components produced by Worden. Both types of elements are made of fused quartz which by virtue of its $4.0 \times 10^{-7}/^{\circ}C$ coefficient of linear expansion renders the sensors insensitive to normally encountered variations in ambient temperature. The use of fused quartz allowed extremely fine suspension fibers (1 mil,) to be employed which enabled the instrument to obtain maximum sensitivity, while still having the strength for reasonable portability. In actuality, the tiltmeter elements survived air freight shipment from Houston. The fused quartz, while beir.g subject to sudden fractures due to its negligible yield, proves to have excellent qualities for this type of work. It can be cut, drawn, and welded with considerable ease into almost any form. The Worden firm has the talent of being able to form 1 mil. quartz fiber into zero length

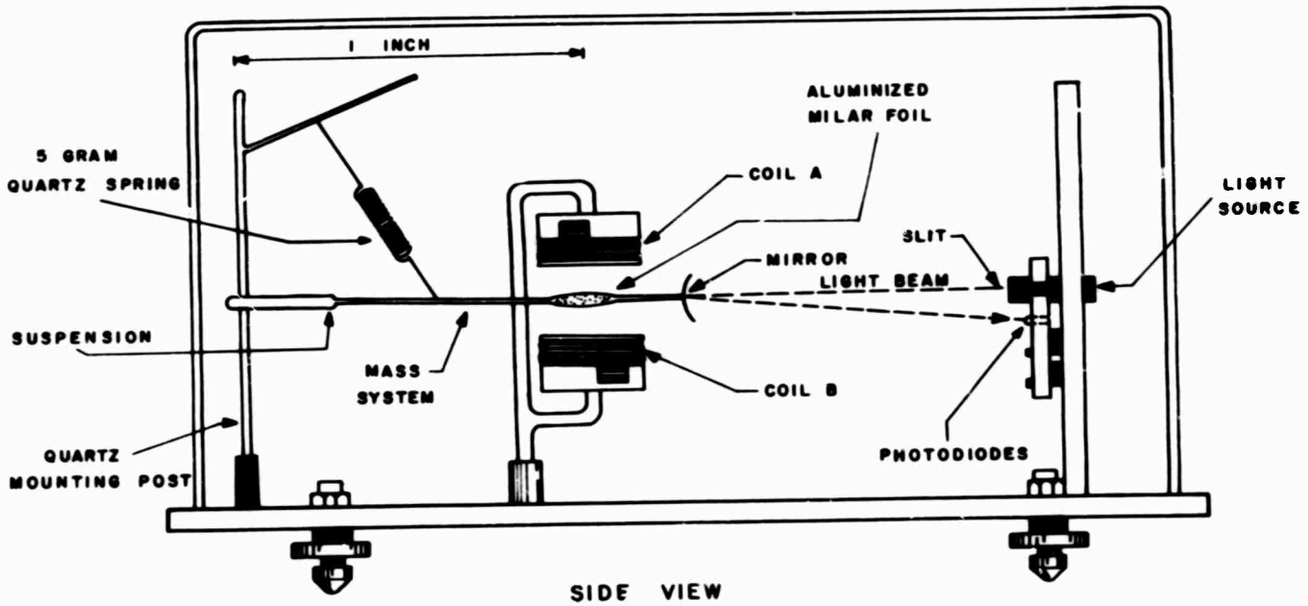

SIDE VIEW

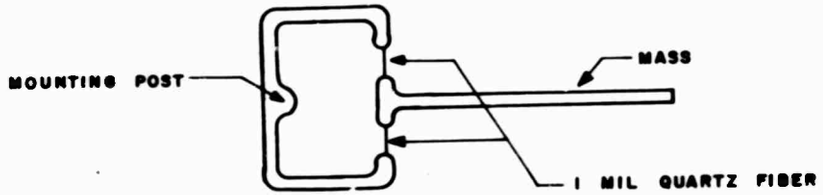

TOP VIEW SUSPENSION DETAIL

GRAVIMETER MECHANICAL DESIGN

FIGURE 27

69.

TILTMETER MECHANICAL DESIGN

FIGURE 28

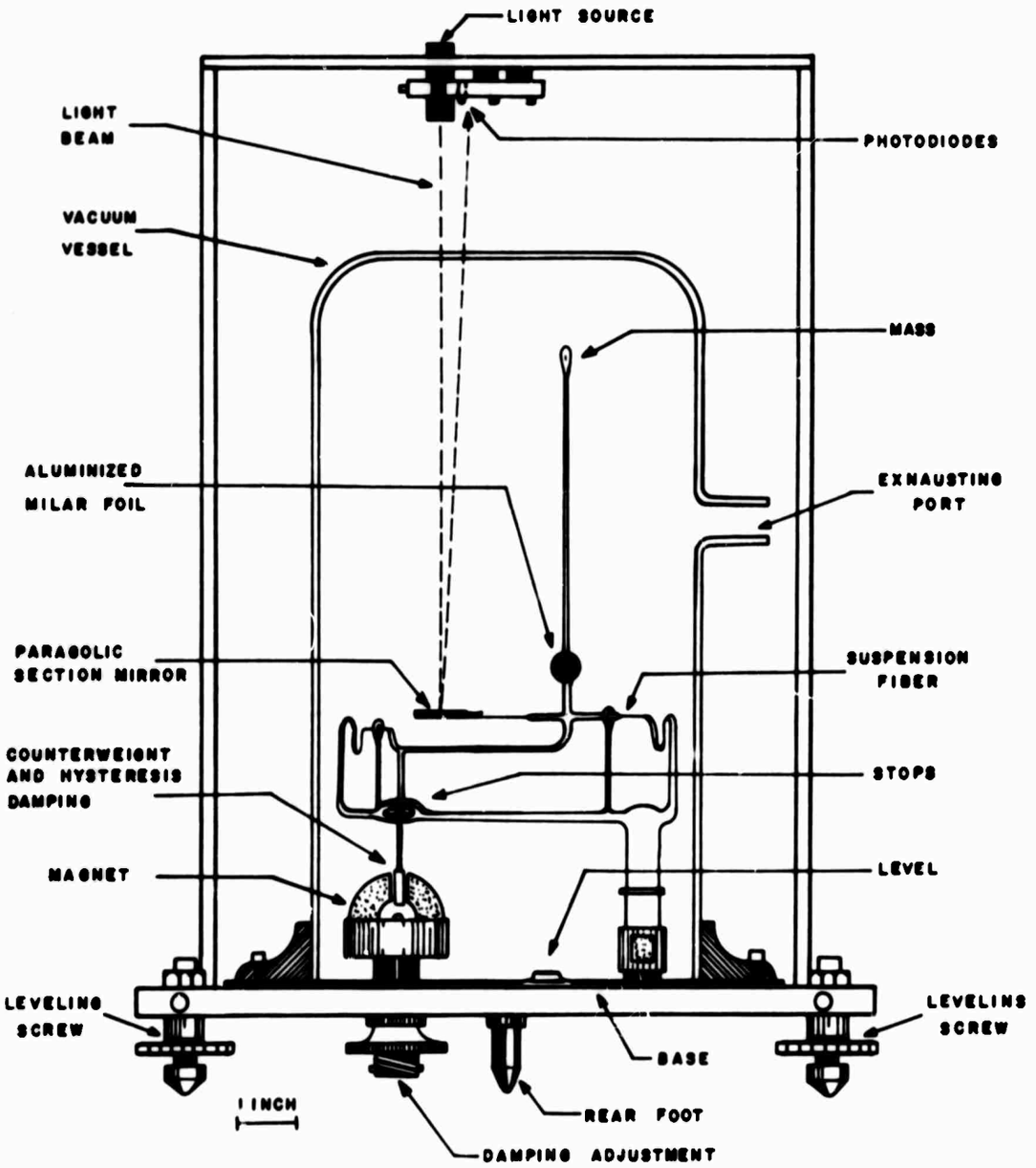

SIDE VIEW — DRIVE COILS REMOVED

TILTMETER MECHANICAL DESIGN

FIGURE 29

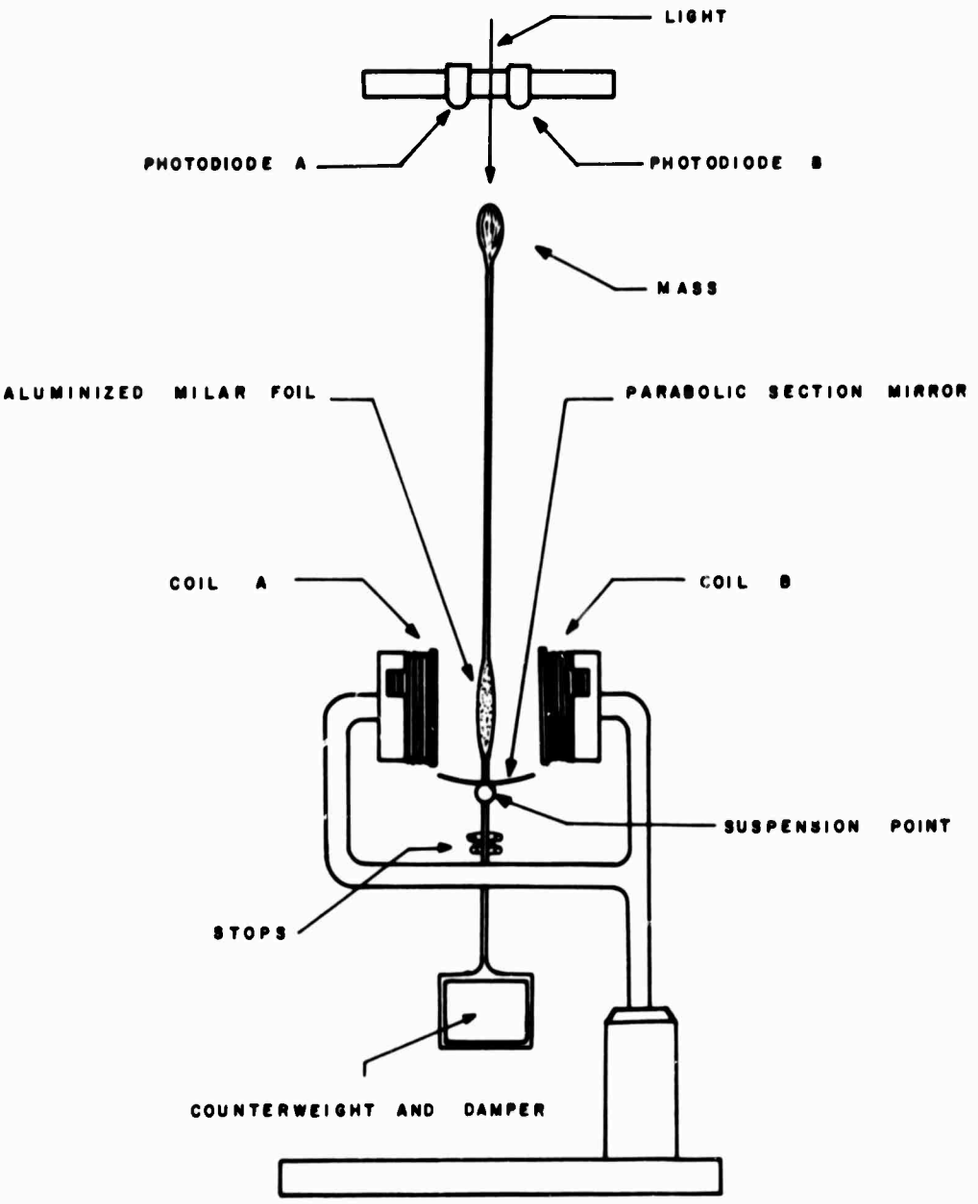

END VIEW — DAMPING MAGNETS REMOVED

CASE I - ZERO POSITION

FIGURE 30

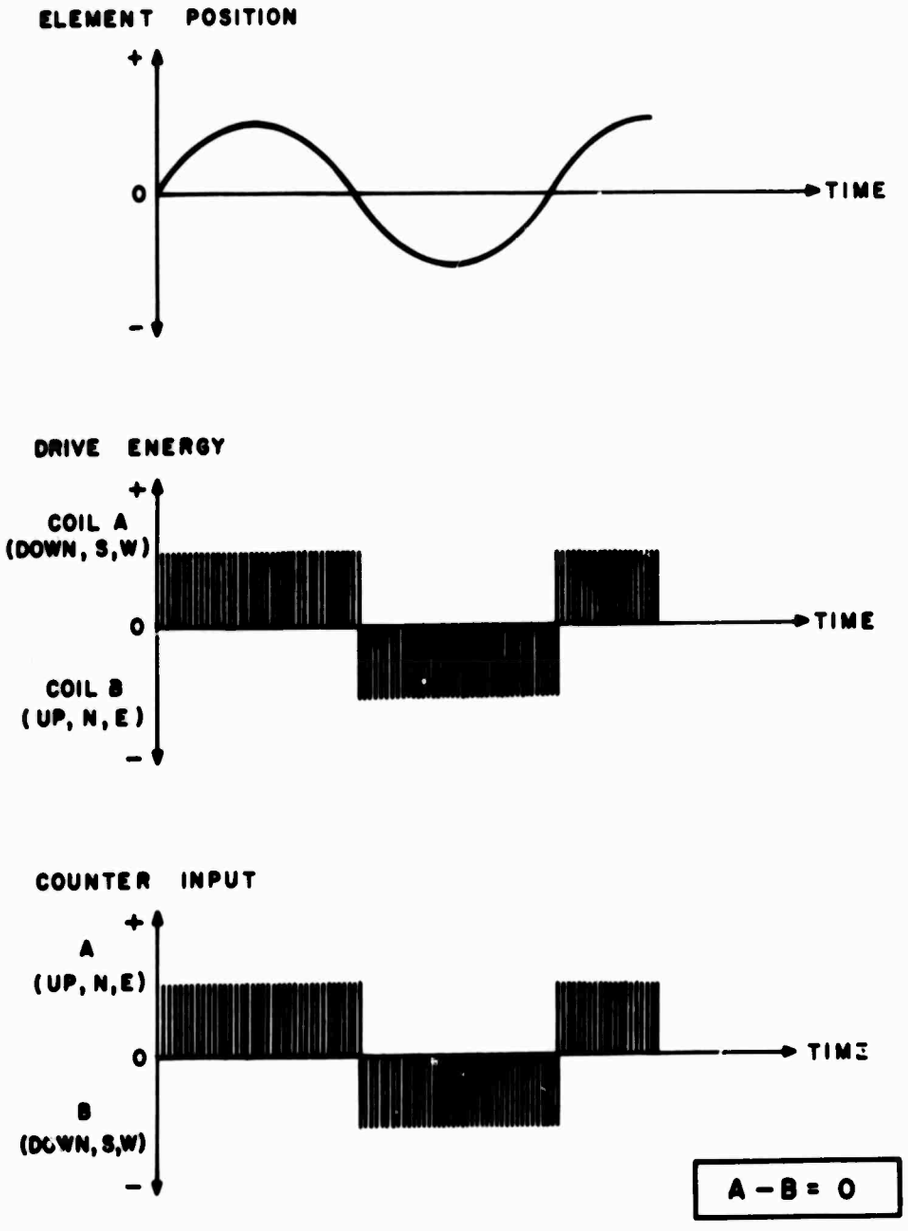

CASE II - GRAVITY DECREASED, TILT NORTH OR EAST

FIGURE 31

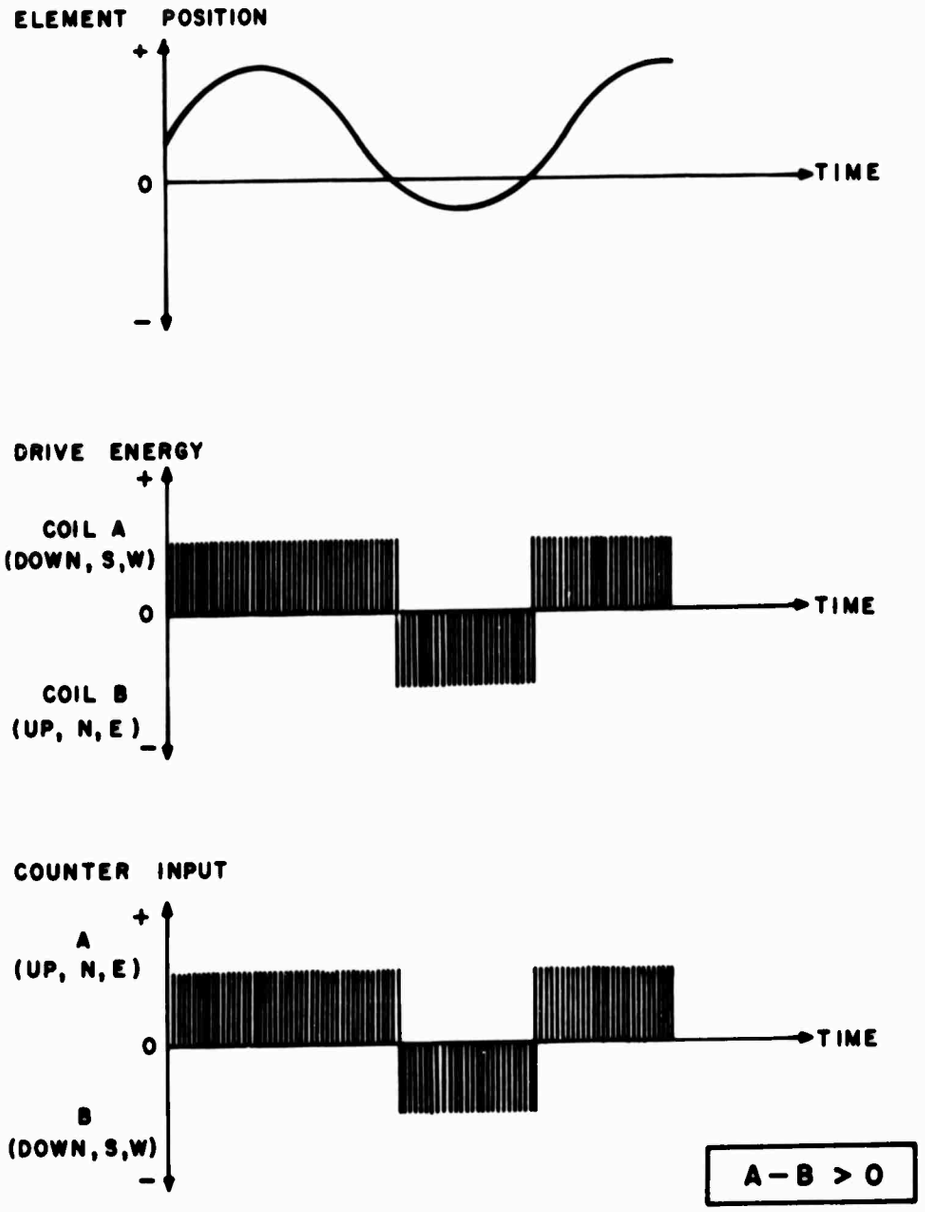

springs with repeatable elastic constant. All of the quartz work was done with a miniature oxygen-propane torch, using medical grade gases to prevent plugging of the small torch orifice.

The elements have been fitted for operation in a moderate vacuum of approximately 1_{μ} to reduce buoyancy effects, convection current interference, Brownian motion, and to prevent imbalance due to condensation of moisture on the elements. Initial tests indicate that the sensors can be completely disconnected from the pumping system for up to a month without appreciable admittance of air, thus preventing any interference from the mechanical pumps and increasing the system portability.

One major problem encountered in working with the elements was the accumulation of electrostatic charges biasing the zero position. This problem was rectified by depositing an alpha emitting radium acetate powder on a mylar substrate and placing a piece of this material within each vacuum vessel. The alpha emission efficiently creates sufficient ionization to remove any static buildup. In the event of a static buildup on the outside of the vacuum vessel, an alcohol wash provides the correction.

Each sensor is provided with precision adjustment screws to position the reference zero point in the center of the instrument's range.

The light sources for the sensors use long-life constant output incandescent bulbs operating from current regulated power supplies. The photodiodes were selected for high light to dark resistance ratio and were matched for equal performance to balance the circuit. The servo coils consist of #36 AWG enameled wire wound onto Ferroxcube Corp. 3B9 arsenic free ferrite forms to a DC resistance of 16 Ω. The pulse servo energy is delivered to a 3/8" disc of aluminized milar foil on the sensor element by interaction of the magnetic field of the coils and the resulting magnetic field set up by the induced eddy currents in the foil. The use of induced currents in the foil rather than direct ferromagnetic repulsion prevents any instabilities due to remnant magnetization.

Figure 32 shows a block diagram of the electronic circuitry. This circuit is compatible with either a gravimeter or tiltmeter element and conceivably could be commutated between a set of three sensors. The circuit is wired on printed circuit boards and filed within the Atec counter which in turn provides the regulated ± 12 volt power.

The first stage is a differential Darlington current amplifier with adjustable input threshold which greatly magnifies the resistance variations of the photodiodes. This is followed by a low pass filter

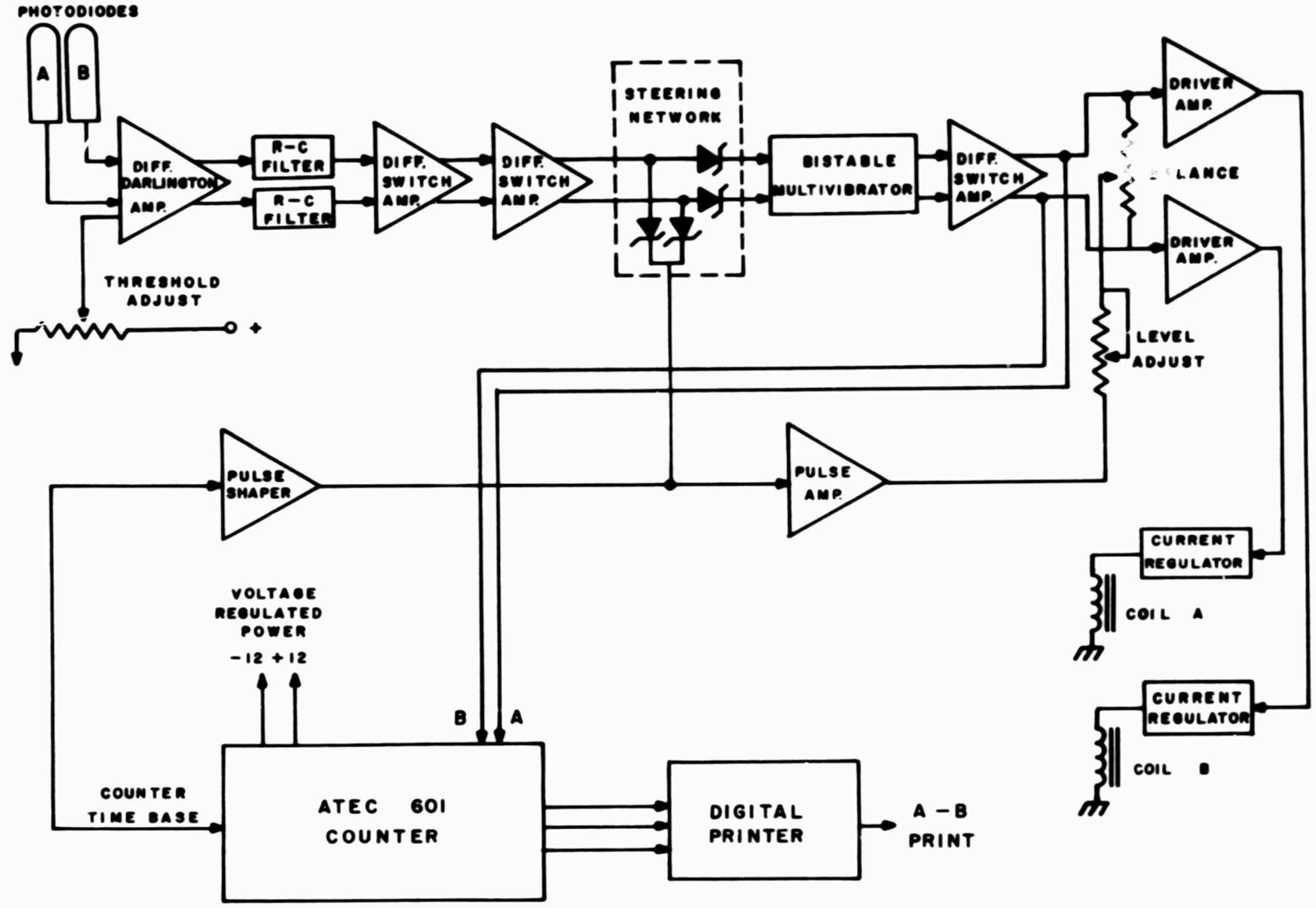

GRAVIMETER - TILTMETER ELECTRONICS

FIGURE 32

which serves to dampen the system's response to any high frequency resonances of the sensor element parts and suppresses any transients which may have been picked up by the cables connecting the electronics to the photodiodes on the sensors. The following two stages are differential switch amplifiers with a negative feedback from the "on" transistor applied to the "off" transistor through the common emitter circuit. This feedback arrangement promotes rapid and positive switching between states. The differential output of the second stage is used during the change of state interval to trigger a bistable multivibrator. At this point the introduction of pulses derived from the counter time base through a pulse shaping amplifier insures that the switching of states occurs in phase-lock synchronism with the counter time base, and thus with the application of pulse energy to the servo coils and the differential counter. The multivibrator in turn determines the state of the following differential switch amplifier and coil driver amplifiers.

The two state nature of the multivibrator serves to prevent the sensor from "hanging up" in the zero position since energy will always be switched to one of the two coils to start the element moving. Adjustments are provided for both pulse height and differential balance in the coil driver circuits. Field effect

current regulators have been added to the coil circuits to prevent any variations of the amplitude of the sensor oscillations due to changes in the driver circuit parameters.

The Atec counter computes the A-B count during the specified integration period and converts the decimal result to an 8-4-2-1 binary code which is then delivered to either a digital printer for a digital record or to a D-A converter for a range-scaled analog record. The counter has the interesting feature of having a double register so that its reset and recycle time is essentially zero. However, since it also senses an enabling level from the coil driver electronics, it will begin its integration period only as the sensor element passes through its zero position.

Even though the quartz elements are quite insensitive to temperature variations, the possibility that small expansions or contractions of the sensor mounting or adjusting hardware might introduce some drift suggested that a controlled temperature environment would be desirable. For this purpose glass wool insulated wooden enclosures were constructed along with a temperature controlling circuit. The controller is an AC bridge type (Malmstadt and other, 1965) and is shown in Figure 33. The error signal of the AC bridge varies proportionally with the change in the thermistor which

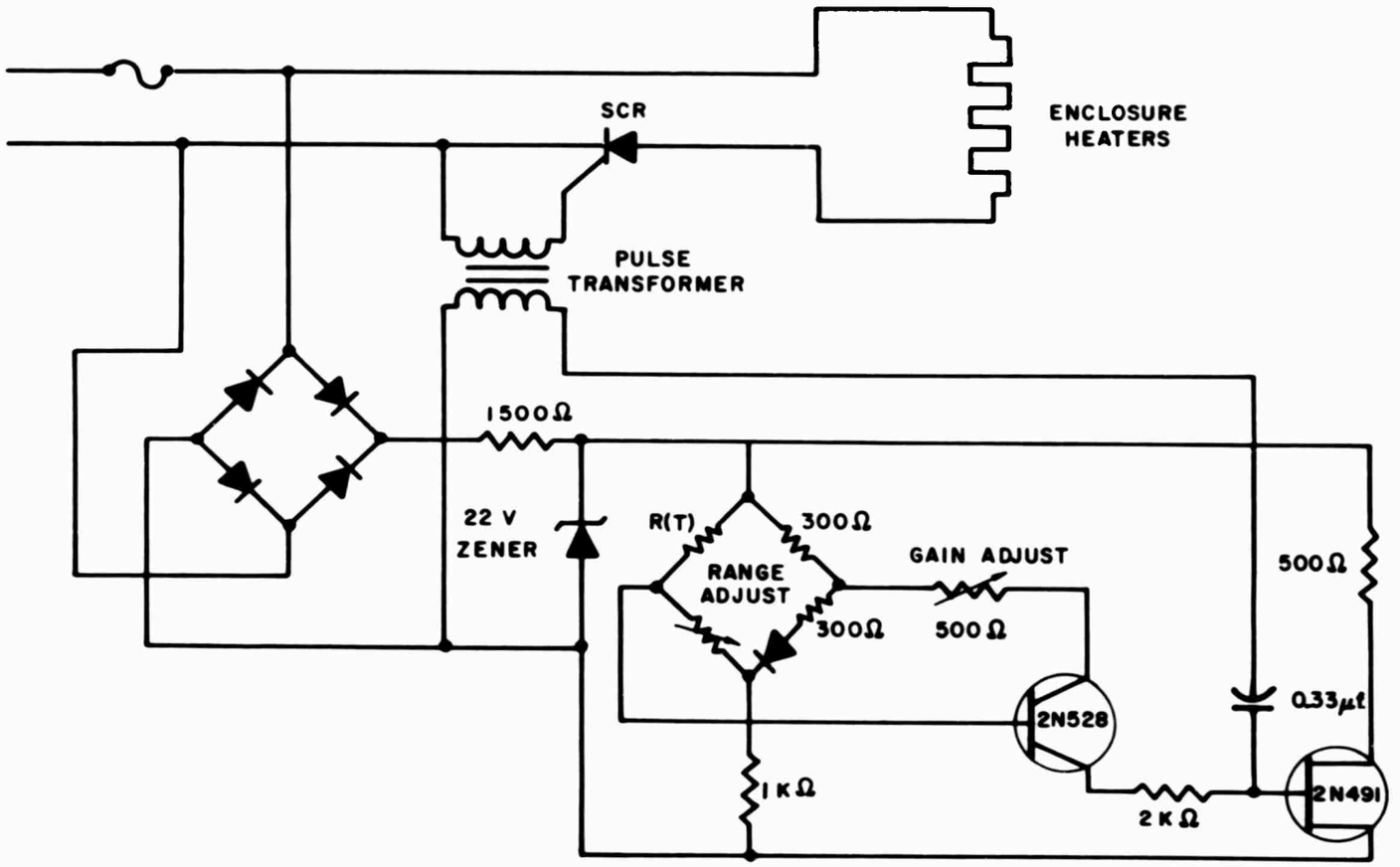

TEMPERATURE REGULATOR CIRCUIT

FIGURE 33

is located on the sensor. This error signal is amplified during the positive half cycles of the power line and the amplified current flow is used to charge a capacitor at a rate determined by a limiting resistor. The rate of charge is proportional to the error of the AC bridge. When the voltage across the capacitor reaches a value determined by the circuit parameters, the unijunction transistor conducts as a relaxation oscillator, discharging the capacitor through the pulse transformer and thus delivering a firing trigger to a silicon controlled rectifier in series with the enclosure heaters. The period of the SCR conduction will in turn be proportional to the error signal in the AC bridge and will be varied in accordance with the amount of heat input required to compensate for a change in the enclosure temperature. Tests have shown that the temperature of the enclosure can be held within $\pm$ 0.5 degrees over a variation of the ambient from 40 to 80^{o}F. These tests were made using an inexpensive and, therefore, low quality thermistor. Finer control would be obtained from a thermistor with a larger $\delta R/\delta T$ ratio.

To evacuate the sensor chambers a vacuum system has been built. A Central Scientific Company Megavac two stage mechanical pump produces vacuum down to 1μ. A two inch Consolidated Electrodynamics, Inc. oil diffusion pump extends the capability to below 0.01μ. The system has been constructed for portability and,

if so required, can provide continuous pumping on three or more sensors.

Since the quantity actually measured in the output of the gravimeter-tiltmeter system is time and is not directly an acceleration in the case of gravity or an angle for tilt, the instrument produces relative results which must be equated to the desired quantities by means of an input calibration. In the case of the gravimeter the optimum method of calibration would be to compare the counter totals at several first order absolute gravity stations. By so doing, a difference in known gravity can be measured in terms of a difference in count, allowing the increment of gravity per count to be determined. Once this is done an electrical bias may be periodically applied to one of the drive coils as a preset calibration pulse. A method of calibration which can be employed without moving the system is accomplished by tilting the sensor. The torque from the force of gravity is maximized when the sensor element is in the plane defined by its two suspension points and its center of gravity is perpendicular to the local gravity vector. If the sensor is tilted relative to this, the instrument will respond to $g \cos\theta$, where θ is the angle between the normal to the new operating plane and local gravity. The resulting change in g as

seen by the instrument is $\delta g/g = -\delta\theta^2/2$. Thus by tilting the gravimeter by a known angle, a known change in system input can be introduced. An alternate method of calibration is to employ the free air gravity correction. Since the free air gravity gradient, $-2g/r$, is -0.09406 milligals per foot (at sea level), the instrument may be calibrated by changing its elevation in free space. This method presumes that the test area is known to be free of disturbing effects on the vertical gradient. This method should also serve to establish a limit of instrumental sensitivity. As of this writing these calibrations have not been performed, since the gravity sensor has just recently been made operable.

In the case of the tiltmeters calibration can be effected by the introduction of known tilts into the sensor through the adjusting screws on the sensor base. Since the adjusting screws have been precision machined, an easily measured fraction of a turn will increment the sensor by a known amount. The increment of angle $\delta\theta$ is expressed by

$$\delta\theta = \tan^{-1} (2N/\sqrt{3}\ lt)$$

where N is the number of turns of the adjusting screws, l is the distance between the equilatorally positioned sensor footings (5.650 inches), and t is the thread of the adjusting screws in

turns per unit length. Currently the sensors are equipped with 18 t.p.i. screws, but the addition of a micrometer adjustment would be desirable. As in the case of the gravimeter, an electrical input to the drive coils may be added to provide a preset calibration pulse.

4. RESULTS AND INTERPRETATION

4.1 Recording of Data

While implementing the actual system hardware from the design specifications, the various components were put into use as soon as they became operational. This was done for two purposes: first, to provide information regarding the functioning of the system; second, to study the geophysical phenomena as they are reflected in the system output.

The compilation of data by the entire system was limited by the availability of recording equipment and delays in obtaining some of the system components, especially the gravimeter element. As a result it was decided to restrict the long term recordings to the North-South component of earth tilt, thus permitting one tiltmeter element and the gravimeter to be free for continued development and short term testing. Beginning in November, 1967, such recordings were made. At first the sensor was used as originally delivered; that is, as a static analog device with the differential voltage of the beam splitter being amplified and recorded, and without a vacuum. For the most part these first tests proved quite unsatisfactory. As other system components became available, they were included into the recording system. One result of this approach was

rather poor continuity of data due to frequent changes, but a careful record of all changes helped to reduce this problem. With the exception of three weeks in March, 1968, all recording was done with the sensor placed on the test pier in the main observatory building. During March, the sensor was placed on a seismic pier about 300 feet northwest of the main observatory building. This pier is located in a highly insulated enclosure, and for this reason and because this location was more removed from civilization noises such as vehicular traffic in the observatory parking lot, etc. a lower noise level was anticipated. However, this pier proved entirely unsatisfactory for recording of earth tilt at high sensitivity because of continual shifting of the pier. This problem may be attributed to the effect of a seasonal change in ground frost which was occuring during this period.

As previously noted the tiltmeter is calibrated by incrementing the sensor frame by a known angle. The frame is equipped with three equilaterally spaced legs, two of which are fitted with adjusting screws, permitting adjustment in both the component direction and the perpendicular direction. Both adjusting knobs have twelve detents on the perimeter. Therefore, after leveling the frame in the direction perpendicular to the measured tilt component,

both screws were turned by the distance between two detent positions of 1/12 of a turn. This resulted in an increment of 3.3 arc minutes or 9.6×10^{-4} radians. This calibration was repeated several times per week during the recording period with no discernable variation in the system output ($< 1\%$).

The output of the tiltmeter can be related to a change in the angle between the sensor frame and hence the pier upon which it is placed, and the direction of the local gravity vector or local vertical. The variations of the output at any given frequency are proportional to the variation of angle or tilt at that frequency plus some equivalent rate of tilt at that frequency due to some source of noise acting upon the system. The anticipated power spectrum of the recording called for a larger power density at the tidal frequencies, but analysis of other portions of the spectrum were desired to study conditions affecting the instrument both internally and externally.

4.2 Data Reduction Methods

Chosen for continuity, the record of North-South earth tilt for February 21 to February 28, 1968 and April 5 to April 9, 1968 were analyzed to determine their harmonic components. The digitized system output was entered for storage on the magnetic tape of the

LINC (Laboratory Instrumentation Computer) at time increments of five minutes. The data was transferred from the prescribed blocks of LINC tape to the input of the Bay State Electronics, Inc. Model 601 Statistical Analyzer. In the statistical analyzer a 503 point autocorrelation function of the data waveform function was computed by means of a hard-wired program option. The autocorrelation function was then transferred from the statistical analyzer back to LINC tape.

With the data so processed the Fourier Transform program was called up along with the autocorrelation function from tape storage. This program computes the transform, $P(F) = 2 C(t) \cos 2 ft\, dt$, for a 511 point function using Simpson's Rule (m = 2) to accomplish the numerical integration. Prior to commencement of the transform computation, a one-sided Hanning function (modified cosine) was used to weight the data to reduce the folding effect of transforming a truncated function. With the completion of the program, the 511 point transform function is stored in two blocks of tape which had been allocated for that purpose. From this point the transform was copied onto paper by teletype output. The one-sided transform goes from $f = 0$ to $f = 1/4\,\delta t$ in 511 steps, where δt is the sampling time interval.

Since the autocorrelation function and the power spectral density form a Fourier transform pair, the computer output provides the power spectrum of the input data. This power spectrum provides valuable insight into the functioning of the measuring system and the geophysical phenomena being recorded.

At times, variations in tilt were noticed which appeared to have frequency components in the 1-30 cph band. Because this is a region of proposed future work with the system, the digitized output of 18 of these events was presented to the computer for the same processing as described above. For these higher frequencies a time increment of 1/4 minute was used.

During the course of testing one of the tiltmeter sensors was set up to record seismic disturbances. This was done for two reasons; first, to check various aspects of the sensor design for possible use in seismometers; second, to attempt to determine the extent of system drift from parametric pumping of the sensors. To accomplish this, the system was again set up to operate in a fully analog manner, the differential beam-splitter voltage being amplified and recorded with no servo drive applied to the sensor element; and a relatively high recording speed was employed. In order to study

the microseismic response of the instrument, the amplified beam-splitter voltage was delivered into the Bay State Statistical Analyzer. Here by means of a high speed analog to digital converter and the hard-wired program, a 503 point autocorrelation function of the output function of the sensor was computed using a δt of 0.33 seconds. The autocorrelation function was then transferred to the LINC for harmonic analysis following the procedure as previously described. In addition to microseismic activity, several larger disturbances were recorded. The best recording obtained due to advanced warning is of surface waves from a high yield underground thermonuclear explosion at Pahute Mesa, Nevada.

In obtaining information about the functioning of the electronic portions of the system, full use was made of the facilities of the Weston Observatory electronic laboratory under the supervision of Mr. Hansen. All measurements are National Bureau of Standards traceable.

4.3 System Performance

In the testing of the gravimeter-tiltmeter system, an effort was made to determine the type and extent of error and noise sources encountered in the instrumentation itself. The main souce of error to the digital system is variations in the amplitude of the driven

oscillations of the sensor elements. When the sensors are oscillating asymmetrically with respect to the zero position, any change in amplitude will result in a change of the time of the zero crossing, thus contributing error to the counter output. This is equivalent to jitter, and is the mechanism by which several noise sources introduce error to the system. The system noise sources were found to lie in the following areas.

1. Electronics:

Noise error in the electronics can be generated in two locations. The first is in the photodiode sensing circuit. As previously noted the circuit includes a bistable multivibrator which is preceeded by a differential Darlington amplifier and two differential switch amplifiers. It is the characteristic of the multivibrator because of its regenerative action that it will switch to the state determined by the larger of the two inputs. The actual voltage difference discriminated by this multivibrator has been determined to be less than 10^{-5} volts out of a possible maximum difference of 8 volts. However, drifts in the preceeding stages can effect the point of discrimination. To reduce this problem the following steps have been taken:

1. Use of matched high sensitivity photodiodes on the sensing elements.

2. Use of pre-aged, long life light sources using current regulated power supplies to provide constant input to the photodiodes.

3. Use of shielded leads between sensors and electronics to reduce interference effects.

4. Use of differential amplifier configurations to provide common circuit elements and a stabilizing feedback.

5. Use of silicon semiconductors to reduce thermal changes of circuit parameters.

6. Use of close packaging of components to reduce thermal gradient imbalance.

7. Use of overrated circuit components to reduce aging effects.

8. Use of voltage regulated power supplies.

9. Application of time base pulses to the multivibrator input to phase lock switching action to counter time base.

By following careful design policy, the accuracy of discrimination is ultimately limited by the Johnson noise which is proportional to the familiar kTB factor.

The other area in which the electronics can introduce noise error is in the coil driver circuit. Obviously, a variation in the drive energy will change the amplitude of the sensor

oscillations, thus introducing error by the mechanism previously discussed. To reduce this problem the following steps have been taken:

1. Use of arsenic free ferrite drive coils to reduce remnant magnetization.

2. Use of series resistances to reduce current flow and subsequent heating in the drive coils.

3. Use of resistances in parallel with the drive coils to further reduce current flow to the minimum required and divide the effect of current variations.

4. Provisions for balancing the drive level to the two coils.

5. Use of silicon transistors to reduce thermal effects.

6. Use of egulated power supplies.

In addition, field-effect current regulators are being added to further obviate any variations. Throughout the remainder of the electronics the error should not exceed $\pm$1count plus the time base error since the system is purely digital and can operate with signal to noise ratios as low as 1:1. In actuality, the SNR of the digital electronics is high, typically 20:1.

2. Temperature and temperature gradient effects:

Expansion of sensor components and variations in elasticity

of suspension elements due to temperature changes can result in system noise. For this reason quartz was chosen as the structural and suspension material. Since the sensors are mounted on a triangular based footing a uniform temperature variation of the legs would not be noticeable in the form of a tilt. However, in this case a change in the temperature gradient between any two legs would produce a change in the system output. To reduce temperature and temperature gradient effects the sensors have been provided with a temperature controlled environment as previously noted. Rather than introduce heat at one point in the enclosure, a separate heating element was placed in each corner of the enclosure to reduce gradients. Also, with this purpose in mind, the enclosure was insulated so that the required heat input is small. The effects of a varying temperature gradient across the test pier has been considered. The expansion of concrete is moderate ($8 \times 10^{-6}/^{o}C$) and integrated over the substantial vertical thickness of the test pier, a change in the horizontal gradient would tilt the top surface of the pier. In view of the large mass of the pier, such changes are difficult to measure due to the long time required to change the heat content of a section of the pier. However, to reduce the application of a heat source to the

pier, the temperature of the enclosure is maintained only several degrees above the highest ambient encountered, and the pier room is kept closed to help regulate the ambient temperature. The desirability of "baking" the sensors at temperatures of several hundred degrees has been discussed, but has not been followed because of this suspected effect on the test pier.

3. Pressure effects:

Air molecules within the sensor contribute significantly to the element damping by frictional and buoyancy effects. As a result variations in the barometric pressure around the element will affect the amplitude of the driven oscillations of the element, thus introducing errors as previously discussed. As noted, the sensor chambers are evacuated to about 1_{μ}, sealed, and removed from the pumping system. Because of equipment limitations, it has not been possible to monitor the pressure within the chambers, and it seems obvious that the chambers have some leak rate. Thus over a period of time the internal pressure wili be changing, introducing some degree of error. There appear to be three alternatives in solving this problem. The first is to operate the sensors at atmospheric pressure. This introduces uncertainties due to fluctuations of the atmospheric pressure and effects due to variations in moisture

content and condensation. The second alternative is to use improved chambers employing pressure monitoring equipment. This approach may be employed in subsequent models of these types of sensors. The third alternative is to employ continuous pumping on the sensor chambers. In the case of the tiltmeters, this will require a vacuum connection which will not introduce any motions onto the sensor frame.

4. Tilt and gravity effects:

As noted in the section on calibration of the gravity sensor, the gravimeter element is sensitive to tilts, geophysical or instrumental. Since $\delta g/g = - \delta \theta^2/2$, the effect is of second order in θ, or for 10^{-6} radians is of order 10^{-12}g. Instrumental tilts are reduced by the controlled temperature environment as previously noted.

The tiltmeter elements sense the direction of the local gravity vector and compare it to the local platform attitude. It then becomes necessary to investigate the effect of a change in the magnitude of the gravity vector. As soon as a torsion is supplied to the suspension fibers, the element will not be perfectly aligned with the local gravity, but will seek equilibrium between

the torque generated by gravity and the restoring torque of the suspension fibers. Thus a variation in gravity would result in a change of the equilibrium point. This effect has been calculated to be a second order effect of the elastic constant of the torsional suspension, and since the elastic constant of the 1 mil. quartz is very low (10^{-7}), the effect proves to be negligibly small (10^{-12} rad./milligal).

5. Magnetic Field Effects and EMI:

Since magnetic fields are employed to drive the sensor elements, a variation in the ambient magnetic field can buck or reinforce the field developed by the drive coils. This would in turn affect the amplitude of the sensor element oscillations and introduce error by the mechanism previously mentioned. Worse case estimates for a 10^{-2} gauss field change during a geomagnetic storm indicate an error of order 10^{-9} g or 10^{-9} radians. In the event that magnetic disturbances introduce more serious noise than estimated, mu-metal shielding can easily be incorporated into the sensor enclosures to provide a magnetically stable environment.

Electromagnetic interference has already presented problems in the system operation. The primary source of trouble

is 60 Hz energy picked up in cabling ground loops. The other source is the modulation envelopes of RF transmissions introducing errors into the digital system. Both sources of interference have been satisfactorily eliminated by proper use of shielding. However, because of pickup on the cabling from the sensor photodiodes to the electronics, it may prove necessary to locate the first stage of amplification at the sensor, or to increase the common mode rejection ratio of the first stage amplifier, when longer length interconnecting cables are employed.

6. Parametric pumping:

The sensor elements are known to respond to energy of the normal seismic background. This response is both that of the entire element with a magnification curve centered around the natural frequency, and parasitic oscillations of the various parts of the sensors at the various parasitic frequencies. In the event that any of these responses is non-linear, it can parametricly pump or rectify the high frequency seismic energy into an energy band approaching zero frequency. Since the microseismic energy usually arrives in groups, it is expected that this parametric pumping will introduce noise energy at the group repetition frequency.

Also a slow build up of microseismic activity will result in a corresponding slow drift of the instrument. Since the non-linear response characteristics or the sensor elements are not known, no attempt has been made to estimate the magnitude of this effect; however, it is intuitively felt that at times of high microseismic activity the contribution of this noise source may be significant. The normal linear response of the sensor elements to the microseismic activity is attenuated in the system output by the low-pass filter action of the integrator.

7. System linearity:

The linearity of the digital system is a function of the driven oscillation of the sensor elements. If the oscillation is a pure sinusoid, the output will not be linear across its range; the sensitivity will rather have a cosine taper function due to changes in slope of the oscillation curve. With adjustment of the drive power and damping, the oscillation can be made to more closely approximate a triangular wave. For the triangular wave on which the slope remains constant on each half cycle, the instrument will be linear across its entire range. However, since the amplitude of the oscillation is considerably larger than the deflection produced

by a geophysical variation in tilt or gravity, the normal change in system output will be a small portion of the total range and the required linearity correction is small.

4.4 Geophysical Observations

Figure 34 shows the power spectral density of variations in North-South tilt as observed on the test pier at Weston Observatory. The result is obtained from the transform of the autocorrelation of data from two recording periods as previously noted. Two distinct peaks are observed at the tidal frequencies of 12 and 24 hours respectively, although both far exceed the predicted tidal values. The twelve hour component, being the fundamental of the oceanic tide as well as earth tide, is most probably due to tidal loading on the sea coast which is about twelve miles from Weston, rather than purely the earth tide. The predominant 24 hour component, by virtue of its amplitude is clearly not earth tide, but rather is the effect of insolation produced surface tilts. This effect also shows by the presence of a 48 hour component. This component will arise from variations in the amplitude of the insolation tilt with cloud cover; that is, a sunny day followed by a cloudy one will produce a 48 hour

POWER SPECTRUM - NORTH-SOUTH EARTH TILT
SEISMIC TEST PIER, WESTON OBSERVATORY

FIGURE 34

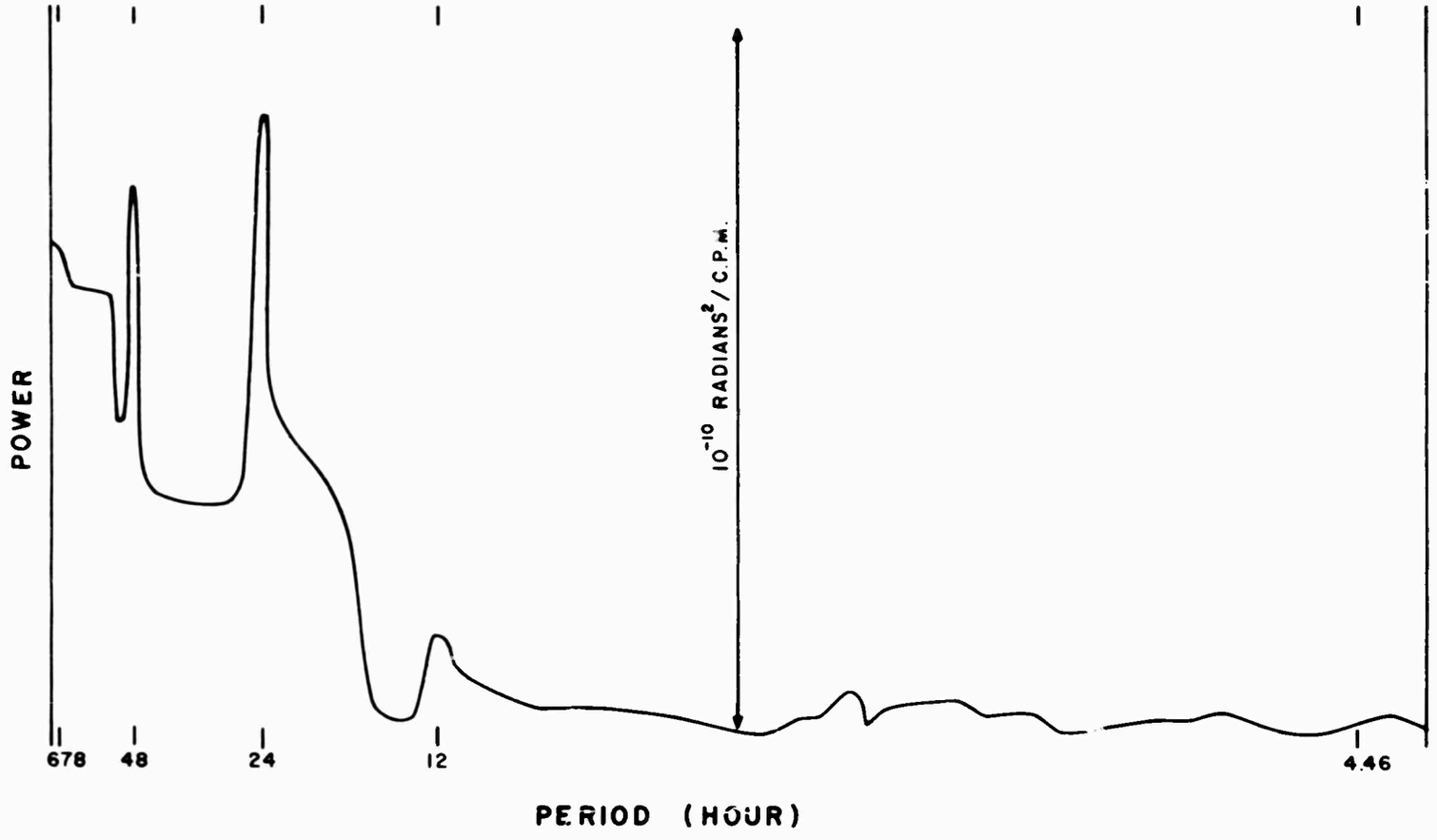

component. Examination of the tilt records shows that the amplitude of the 24 hour component does reflect variations in the meteorological conditions, and a general increasing trend is noticed reflecting the increase of solar zenith angle and daylight hours during the recording period. Also, during the time while recordings were being made was a period of several days of heavy rain. The result was a highly erratic tilt recording indicating the effect of ground water on surface tilt.

Figure 35 shows the power spectral density of variation in North-South tilt at higher frequencies. The result is obtained from the transform of the autocorrelation of data from a series of isolated events which by visual appearance were determined to contain high frequency components. Since the number of spectral peaks is large compared to the number of events processed, it would be unrealistic to conclude that this is a representative power spectrum. Therefore, for lack of additional data, it is presented for comparison with the results from a more representative sample.

Figure 36 shows the power spectrum of the microseismic response of the tilt sensor. Predominant in the spectrum is the sharp peak at the fundamental frequency of the sensor. This

POWER SPECTRUM — HIGH FREQUENCY EARTH TILT
SEISMIC TEST PIER, WESTON OBSERVATORY

FIGURE 35

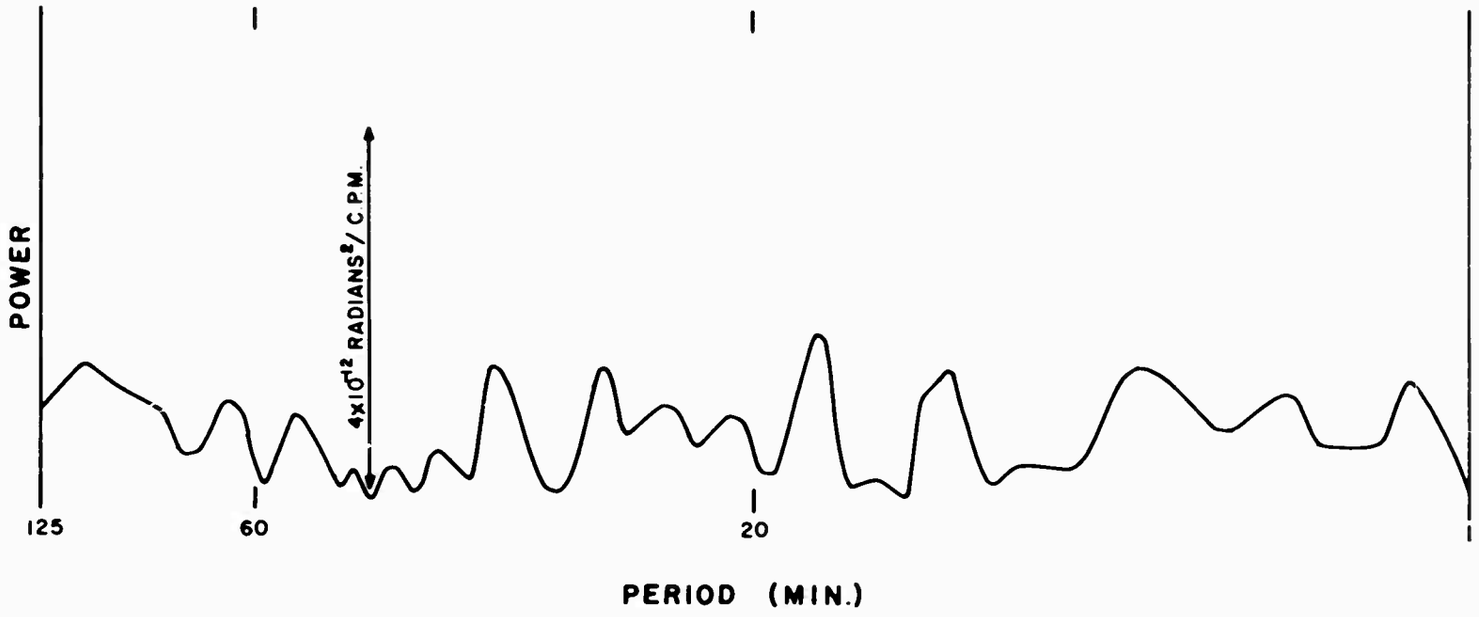

POWER SPECTRUM OF INSTRUMENTAL MICROSEISMIC RESPONSE

FIGURE 36

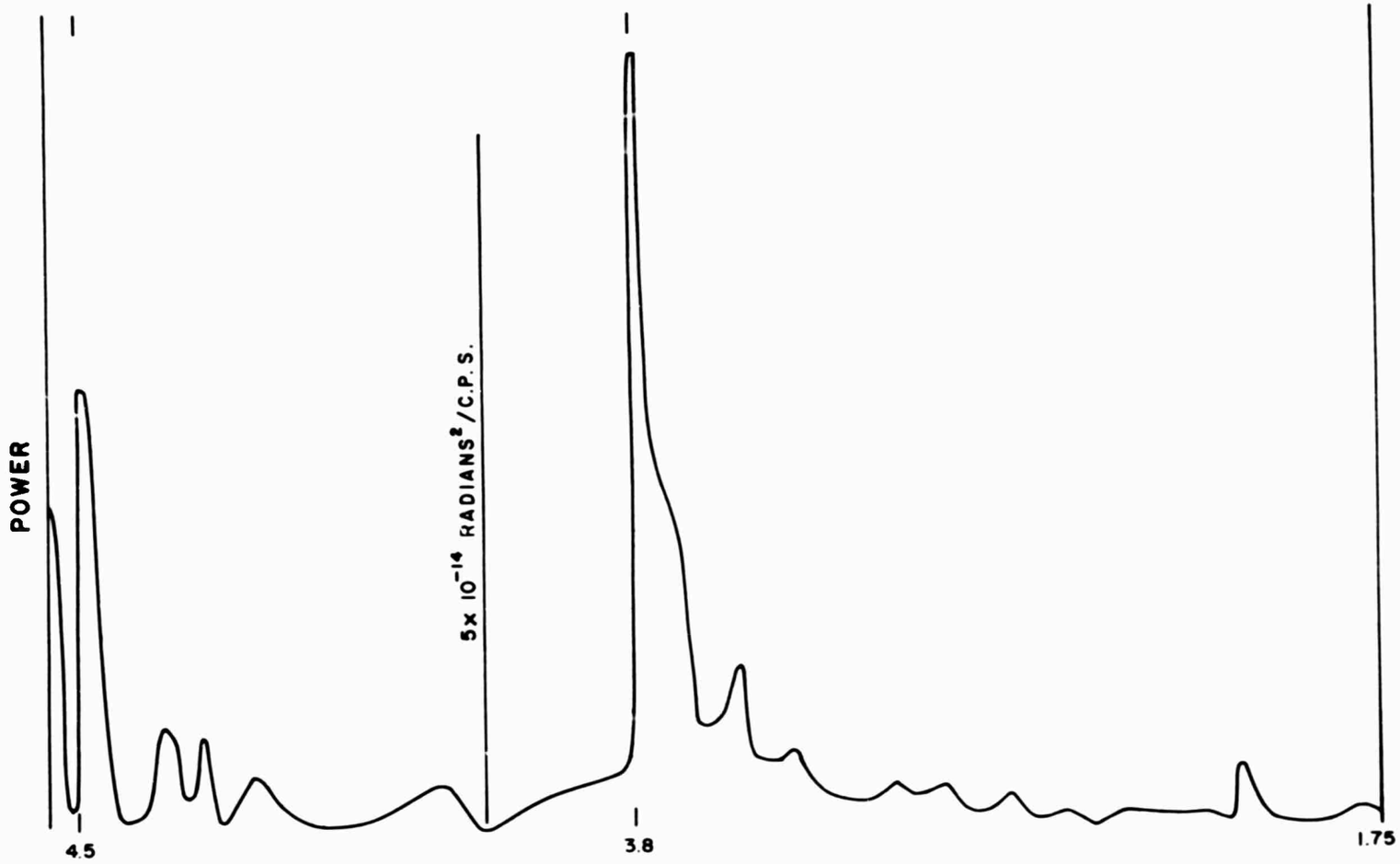

indicates a high mechanical Q or narrow band response. Thus if this basic type of sensor is to be applied as a seismometer, provisions must be made to broaden out the response band pass either by change in mechanical design or by dissipation of more energy by a more effective damping mechanism than is currently provided. The peak at 47 seconds/cycle is either a long period microseism or the microseism group frequency. A record of surface waves from an underground nuclear explosion is shown in Figure 37 . The narrow band-pass seismic response of the instrument is evident from this record. The calibration of the record is given in equivalent tilt; however, the instrument is responding both to actual tilts and horizontal accelerations.

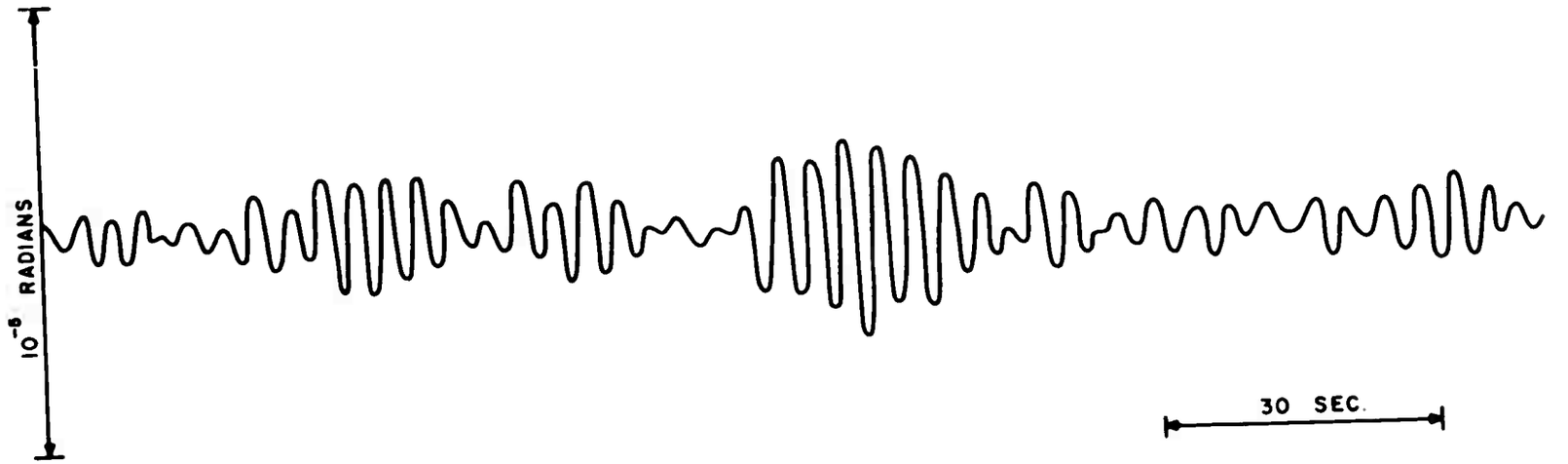

SURFACE WAVES FROM AN UNDERGROUND NUCLEAR EXPLOSION AT PAHUTE MESA, NEVADA

FIGURE 37

BIBLIOGRAPHY

Alsop, Leonard E., Sutton, George H., Ewing, Maurice
"Free Oscillations of the Earth Observed on Strain and Pendulum Seismographs", Journal of Geophysical Research (66) No. 2, pp 631-641, 1961.

Bartels, Julius
Handbuch der Physik, Vol. 48, p 734ff., Springer, Berlin, 1957.

Bendat, Julius S., Piersol, Allan G.
Measurement and Analysis of Random Data, John Wiley and Sons, Inc. 1966.

Benioff, H., Gutenberg, B., Richter, C. F.
"Progress Report of the Seismology Laboratory of California Institute of Technology" Transactions of the American Geophysical Union, (35) pp 979-987, 1954.

Block, Barry, Moore, R. D.
"Measurements in the Earth Mode Frequency Range by an Electrostatic Sensing and Feedback Gravimeter", Journal of Geophysical Research, (71) No. 18, pp 4361-4375, 1966.

Bracewell, Ron,
The Fourier Transform and its Applications, McGraw Hill, 1965.

Clarkson, H. N., Lacoste, L. B. J.
"An Improved Instrument for Measurement of Tidal Variation in Gravity", Transactions of the American Geophysical Union, (37) No. 3, pp 266-272, 1956.

Garland, G. D.
The Earth's Shape and Gravity, Pergamon Press, Oxford, 1965.

Haynes, W. E.
Thesis Submitted for the Degree of Master of Science, Graduate School of Boston College, June 1968.

Heiskanen, W. A., Vening Meinesz, F. A.
The Earth and Its Gravity Field, McGraw-Hill Book Company, Inc. New York, 1958.

Malmstadt, H. V., Enke, C. G., Toren, E. C.
Electronics for Scientists, pp 384-388, W. A. Benjamin, Inc. New York, 1963.

Munk, W. H., MacDonald, C. J. F.
The Rotation of the Earth--A Geophysical Discussion, pp 23-37, Cambridge University Press, 1960.

Ness, N. F., Harrison, J. C., Slichter, L. B.
"Observations of the Free Oscillations of the Earth", Journal of Geophysical Research, (66) No. 2, pp 621-629, 1961.

Okubo, S.
Personal communications, 1967.

Simon, Ivan, McConnell, Robert K., Jr.
Arthur B. Little, Inc., Geophysical Tiltmeter, in-house report, Arthur D. Little, Inc., 1967.

Thompson, Lloyd G. C., Bock, Robert L., Savet, Paul H.
Gravity Gradient Sensors and Their Applications for Manned Orbital Spacecraft, a paper presented at the Third Goddard Memorial Symposium of the American Astronautical Society, Washington, D. C., March 19, 1965.

Weber, Joseph
"Gravitational Waves", Physics Today, (21) No. 4, pp 34-39, 1968.

Unclassified

Security Classification

DOCUMENT CONTROL DATA - R&D

(Security classification of title, body of abstract and indexing annotation must be entered when the overall report is classified)

1. ORIGINATING ACTIVITY *(Corporate author)*
Trustees of Boston College
Chestnut Hill, Massachusetts 02167

2a. REPORT SECURITY CLASSIFICATION
Unclassified

2b. GROUP

3. REPORT TITLE
EVALUATION OF SEISMIC INSTRUMENTS AND BASIC RESEARCH ON SEISMIC WAVE PROPAGATION

4. DESCRIPTIVE NOTES *(Type of report and inclusive dates)*
Scientific. Final. Period Covered: June 1, 1966 - August 31, 1968

Approved 19 November 1968

5. AUTHOR(S) *(Last name, first name, initial)*
John G. Hogan
Joseph J. Blaney
John F. Devane, S.J.
Thomas E. Foley
William E. Haynes
Robert E. Hansen

6. REPORT DATE
October 1968

7a. TOTAL NO. OF PAGES
107

7b. NO. OF REFS
17

8a. CONTRACT OR GRANT NO.
AF19(628)6067 ARPA Order No. 292

b. PROJECT AND TASK NO. Work Unit Nos.
8652-07-01

c. DOD ELEMENT
6250601R

d. DOD SUBELEMENT
n/a

9a. ORIGINATOR'S REPORT NUMBER(S)

9b. OTHER REPORT NO(S) *(Any other numbers that may be assigned this report)*
AFCRL-68-0589

10. AVAILABILITY/LIMITATION NOTICES
1. Distribution of this Document is unlimited. It may be reseased to the clearinghouse, Department of Commerce, for sale to the general public.

11. SUPPLEMENTARY NOTES
This research was supported by The Advanced Research Projects Agency

12. SPONSORING MILITARY ACTIVITY
Air Force Cambridge Research Laboratories (CRJ)
L. G. Hanscom Field
Bedford, Massachusetts 01730

13. ABSTRACT

Seismometer test procedures are presented. Results of the tests performed on Electro-Tech's model EV17 seismometers used in the portable seismic detection system are detailed.

The results of frequency response tests performed on the portable seismic detection system are presented. Changes and modifications of the portable seismic detection system are described.

Equipment additions to the Data Analysis Laboratory are described. A brief discussion of a program used to process data taken with the portable seismic detection system is given.

A description of a quartz fiber tiltmeter and gravimeter developed during this contract is presented.

DD FORM 1 JAN 64 1473

Security Classification

14. KEY WORDS	LINK A		LINK B		LINK C	
	ROLE	WT	ROLE	WT	ROLE	WT
Seismometer Testing						
Portable Seismic Array						
Seismic Data Processing						
Quartz Tiltmeter						

INSTRUCTIONS

1. ORIGINATING ACTIVITY: Enter the name and address of the contractor, subcontractor, grantee, Department of Defense activity or other organization *(corporate author)* issuing the report.

2a. REPORT SECURITY CLASSIFICATION: Enter the overall security classification of the report. Indicate whether "Restricted Data" is included. Marking is to be in accordance with appropriate security regulations.

2b. GROUP: Automatic downgrading is specified in DoD Directive 5200.10 and Armed Forces Industrial Manual. Enter the group number. Also, when applicable, show that optional markings have been used for Group 3 and Group 4 as authorized.

3. REPORT TITLE: Enter the complete report title in all capital letters. Titles in all cases should be unclassified. If a meaningful title cannot be selected without classification, show title classification in all capitals in parenthesis immediately following the title.

4. DESCRIPTIVE NOTES: If appropriate, enter the type of report, e.g., interim, progress, summary, annual, or final. Give the inclusive dates when a specific reporting period is covered.

5. AUTHOR(S): Enter the name(s) of author(s) as shown on or in the report. Enter last name, first name, middle initial. If military, show rank and branch of service. The name of the principal author is an absolute minimum requirement.

6. REPORT DATE: Enter the date of the report as day, month, year, or month, year. If more than one date appears on the report, use date of publication.

7a. TOTAL NUMBER OF PAGES: The total page count should follow normal pagination procedures, i.e., enter the number of pages containing information.

7b. NUMBER OF REFERENCES: Enter the total number of references cited in the report.

8a. CONTRACT OR GRANT NUMBER: If appropriate, enter the applicable number of the contract or grant under which the report was written.

8b, 8c, & 8d. PROJECT NUMBER: Enter the appropriate military department identification, such as project number, subproject number, system numbers, task number, etc.

9a. ORIGINATOR'S REPORT NUMBER(S): Enter the official report number by which the document will be identified and controlled by the originating activity. This number must be unique to this report.

9b. OTHER REPORT NUMBER(S): If the report has been assigned any other report numbers *(either by the originator or by the sponsor)*, also enter this number(s).

10. AVAILABILITY LIMITATION NOTICES: Enter any limitations on further dissemination of the report, other than those imposed by security classification, using standard statements such as:

(1) "Qualified requesters may obtain copies of this report from DDC."

(2) "Foreign announcement and dissemination of this report by DDC is not authorized."

(3) "U. S. Government agencies may obtain copies of this report directly from DDC. Other qualified DDC users shall request through _____."

(4) "U. S. military agencies may obtain copies of this report directly from DDC. Other qualified users shall request through _____."

(5) "All distribution of this report is controlled. Qualified DDC users shall request through _____."

If the report has been furnished to the Office of Technical Services, Department of Commerce, for sale to the public, indicate this fact and enter the price, if known.

11. SUPPLEMENTARY NOTES: Use for additional explanatory notes.

12. SPONSORING MILITARY ACTIVITY: Enter the name of the departmental project office or laboratory sponsoring *(paying for)* the research and development. Include address.

13. ABSTRACT: Enter an abstract giving a brief and factual summary of the document indicative of the report, even though it may also appear elsewhere in the body of the technical report. If additional space is required, a continuation sheet shall be attached.

It is highly desirable that the abstract of classified reports be unclassified. Each paragraph of the abstract shall end with an indication of the military security classification of the information in the paragraph, represented as *(TS), (S), (C), or (U).*

There is no limitation on the length of the abstract. However, the suggested length is from 150 to 225 words.

14. KEY WORDS: Key words are technically meaningful terms or short phrases that characterize a report and may be used as index entries for cataloging the report. Key words must be selected so that no security classification is required. Identifiers, such as equipment model designation, trade name, military project code name, geographic location, may be used as key words but will be followed by an indication of technical context. The assignment of links, rules, and weights is optional.